Review

Hydraulic Fracture Closure Detection Techniques: A Comprehensive Review.

Mohamed Adel Gabry * , Ibrahim Eltaleb , Amr Ramadan , Ali Rezaei , Mohamed Y. Soliman

Posted Date: 9 August 2024

doi: 10.20944/preprints202408.0725.v1

Keywords: Fracture closure; Hydraulic Fracture; Reverse Engineering; Tangent Method; Compliance method

Review

Hydraulic Fracture Closure Detection Techniques: A Comprehensive Review

Mohamed Adel Gabry [1,*], Ibrahim Eltaleb [2], Amr Ramadan [1], Ali Rezaei [3] and Mohamed Y.Soliman [1]

[1] Department of Petroleum Engineering, University of Houston.

[2] ODSI-Energy; Ibrahim.Eltaleb@osdsi-energy.com

[3] Formerly SLB; ali.rezaei.a@gmail.com

* Correspondence: magabry@cougarnet.uh.edu; Tel.: (optional; include country code; if there are multiple corresponding authors, add author initials)

Abstract: This study reviews methods for detecting fracture closure pressure in both unconventional and conventional reservoirs using mathematical models and fluid flow equations. It evaluates techniques such as the Nolte method, tangent method, and compliance method. The investigation relies on observing changes in fluid flow regimes from pre-closure to post-closure, using fluid flow equations to examine the post-closure flow regime effect on the G function. Reverse calculations model pressure decline across synthesized flow regimes, facilitating a detailed investigation of the closure process. The analysis reveals that the tangent method is sensitive to post-closure fluid flow, while the compliance method is less effective in reservoirs with significant tortuosity or natural fractures. The paper recommends assessing natural fractures' characteristics and permeability to identify the source of leak-off before selecting a technique. It proposes integrating various methods for a comprehensive understanding of subsurface formations, combining their strengths for accurate fracture closure identification and better understanding of subsurface formations. The new proposed workflow employs the Continuous Wavelet Transform (CWT) technique for fracture closure detection, avoiding physical model pre-assumptions or simplifications to confirm the results. This approach offers guidance on selecting appropriate methods by integrating different techniques.

Keywords: Fracture closure; Hydraulic Fracture; Reverse Engineering; Tangent Method; Compliance method

1. Introduction

The estimation of minimum horizontal stress is a crucial step in comprehending fracture propagation, and the estimation of reservoir permeability and pressure. The underlying principle behind classical methods for detecting closure events from pressure decay in diagnostic pumping involves combining aspects of well testing and hydraulic fracture analysis. The use of hydraulic fracturing as a tool to enhance the well productivity and determine the minimum principal stress magnitude was first proposed by Clark (1949)[1] and was further explored by various researchers, such as Hubbert and Willis (1957)[2], Godbey and Hodges (1958)[3], Kehle (1964)[4], Haimson and Fairhurst (1967)[5], and Hickman and Zoback (1983)[6]. The process involves pumping fluid at a pressure greater than the fracture pressure to initiate and propagate a hydraulic fracture through the formation, from which the minimum principal stress can be estimated through pressure measurements during and after injection.

These tests are introduced to estimate fluid leak-off parameters, which can be used to determine the leak-off rate of complex fluids like linear gel or cross-linked gel used in conventional hydraulic fracturing in sandstone/carbonate formations. These tests are referred to as minifrac tests (McLennan and Roegiers (1982) [7]) or fracture calibration tests (Mayerhofer and Economides (1993)[8]). These tests were to estimate the efficiency of the fracturing fluid and the minimum horizontal stress mainly based on the G-function introduced by Nolte (1979) [9]. Mayerhofer and Economides (1993) [10] and

 doi:10.20944/preprints202408.0725.v1

Mayerhofer et al. (1995) [11] added modifications to the analysis to remove the filter cake effect and its impact on the fluid leak-off factor.

With the development of shale gas reservoirs, a new test known as the Diagnostic Fracture Injection Test (DFIT) was introduced, utilizing non-wall building fluid instead of cross-linked gel or linear gel. This test is particularly valuable in unconventional reservoirs where flowback for pressure transient analysis is not feasible. DFIT is used to obtain accurate estimates for stress, permeability, and pore pressure (Craig and Brown, 1999)[12]. DFIT has emerged as a crucial technique for characterizing very tight formations, where traditional well testing is challenging. Its conceptual framework integrates techniques from conventional well-test analysis with those from hydraulic fracture diagnostics. The primary application of DFIT is in post-closure analysis, where it provides precise detection and calibration of the minimum horizontal stress profile. This accuracy makes DFIT an essential component of contemporary fracture design processes (Smith et al. (2015) [13]). Unlike minifrac calibration tests that use fracturing fluid, DFIT detects fracture closure by reflecting an average of the minimum horizontal stress across a lower fracture height. This method offers enhanced precision in stress profile estimation, further solidifying DFIT's role in advanced reservoir characterization and fracture design.

In classic well testing, which is focused on fluid production or injection at pressures beneath the fracture gradient, analysis of pressure data facilitates the determination of reservoir attributes such as permeability and skin effect, as evidenced by contributions as discussed by Theis (1935)[14] and Horne (1995)[15]. DFITs operate under analogous physical principles but introduce key distinctions, notably the dynamic nature of fractures, which undergo changes in size, elasticity, and flow characteristics. This dynamic behavior necessitates a nuanced approach to analysis, diverging from the static fracture assumptions prevalent in conventional well-test interpretations. This method amalgamates well-testing and fracturing diagnostics to offer insights into stress, permeability, and pore pressure metrics, leveraging the analytical foundations laid by Nolte (1979)[9] and expanded upon by subsequent researchers.

The analysis of DFIT pressure decay data encompasses two critical segments: pre-closure and post-closure analysis. The pre-closure analysis employs methods primarily to estimate closure pressure and calibrate the minimum principal stress using established techniques by Nolte (1979)[9] . Subsequent developments include the tangent methodology shaped by Castillo (1987)[16], Barree and Mukherjee (1996)[17], and Barree et al. (2007[18]; 2009[19]). Further advancements were made by McClure et al. (2014[20]; 2016[21]) and Jung et al. (2016) [22] who introduced the compliance method, later enhanced by Wang and Sharma (2017) [23] with the variable compliance method. These techniques are pivotal for detecting accurate fracture closure, a cornerstone for successful post-closure analysis, which focuses on determining permeability and reservoir pressure. This study is dedicated to refining pre-closure analysis to accurately pinpoint fracture closure, utilizing the tangent and compliance methods, currently the primary subjects of industry debate.

Post-closure analysis relies on conventional well-testing techniques described by Gu et al. (1993)[24]; Soliman et al. (2005)[25]; Craig and Blasingame (2006)[26], and the linear flow time function technique by Nolte et al. (1997)[27]. The results and effectiveness of post-closure analysis are critically dependent on accurately detected fracture closure, highlighting the significant role of DFIT's dynamic behavior in ensuring the integrity of post-closure evaluations. Fracture closure refers to the pressure point at which the induced fractures created during hydraulic fracturing close or reach their minimum aperture upon attaining an equilibrium state. This closure occurs as a result of the minimum principal stress field acting on the fractures.

The concept of "fracture closure" in geomechanics and reservoir engineering is a nuanced and frequently debated topic, primarily due to its varied and often implicit definitions. This ambiguity stems from the fact that different researchers and practitioners may subtly alter the definition based on the context of their studies or the specifics of their methodologies. For instance, some define closure as the pressure point at which the closure pressure equals the minimum principal stress, suggesting a mechanical balance. This closure occurs because of the minimum principal stress field acting on the fractures. Others interpret closure in terms of fluid dynamics, positing that it occurs

 doi:10.20944/preprints202408.0725.v1

when no fluid remains within the fracture, as implied by Gulrajani and Nolte (2000)[28]. Additionally, there are definitions focusing on the mechanical properties of the fracture, such as when the fracture stiffness becomes infinitely large as per Craig and Blasingame (2006)[26], or more straightforwardly, when the fracture walls physically contact each other. Each interpretation carries significant implications for engineering practices, such as hydraulic fracturing operations or reservoir management. Due to these variations and their potential impact, the term "closure" is often replaced with another term like "contact point" by McClure (2016)[29] to avoid confusion and ensure clarity in technical discussions and documentation. This shift in terminology should be taken in account in the current debate between tangent and compliance methods.

In our analysis, we define fracture closure as the pressure point at which the induced fracture generated during hydraulic fracturing reaches its minimal aperture, achieving an equilibrium state. The stiffness of the fracture increases during this closure process, although it does not become noticeably high if the formation already contains natural fractures in equilibrium. During closure, the fracture faces come into contact, yet a minimal aperture persists due to the roughness of the fracture surfaces and the inherent heterogeneity and presence of natural fractures within the reservoir.

Many studies have been done to study how well different methods work by testing them on simulated data, lab experimental data, and real field data. However, it remains unclear why certain methodologies perform well in certain cases while others do not. That is because of the complexity of the fracture closure process and the lack of physical measurements of the fracture closure process. The fracture network proved to have a significant impact on the pressure falloff response as discussed by Bruno et. al. (2021)[30].

Incorporating natural fractures into the closure process significantly complicates fracture closure. It transforms the dynamics from simple contact between smooth fracture faces to more complex interactions involving rough fracture surfaces, for both natural and induced fractures, which may close simultaneously or sequentially. Some natural fractures become activated and do not revert to their pre-fracture equilibrium state, closing mechanically with reduced or no aperture. Additionally, some of these natural fractures may retain fracturing fluid, resulting in high-permeability natural fractures. These complex interactions are conceptually depicted in Figure 1.

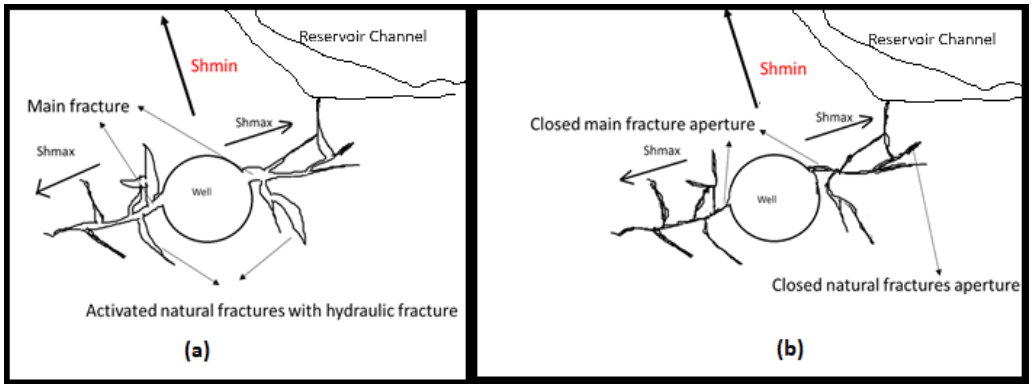

Figure 1. Conceptual illustration of fracture closure dynamics, (a) pre-closure state and (b) post-closure state.

Our research endeavors to synthesize diverse fracture closure detection techniques into a cohesive workflow that melds the physical principles of each method to precisely determine fracture closure for various formation types. This study assesses multiple techniques for identifying fracture closure pressure in both unconventional and conventional reservoirs, using a mathematical model and fluid flow equations.

It examines the strengths and shortcomings of established techniques such as the Nolte method and the tangent method, both employing the log-log technique and compares these to the square root of time technique aligned with the G function and the compliance method, which applies the same G function but from a different perspective on fracture stiffness. The findings indicate that the tangent method is particularly sensitive to post-closure fluid dynamics, while the compliance method is less

 doi:10.20944/preprints202408.0725.v1

effective in reservoirs characterized by extensive far-field tortuosity or the presence of natural fractures.

2. Fracture Closure Detection Techniques

2.1. Nolte (1979)[9] Technique

In his 1979 work, Nolte introduced several fundamental assumptions, including the formation of a single planar fracture, the modeling of leak-off using the Carter leak-off model (Howard and Fast, 1957[31]), and the scaling of fracture growth with time according to a power law. The G-function, a complex expression involving the parameter α, shows only minor sensitivity to variations in α within the practical range of 0.5 to 1.0. Assuming α equals 1.0 significantly simplifies the G-function.

Nolte presented the G-function as a dimensionless time function that correlates shut-in time (t) with pumping time (tp) at an assumed constant rate, derived from the following equations.

$$G(\Delta t_D) = \frac{4}{\pi}(g(\Delta t_D) - g_o) \quad (1)$$

Where $g(\Delta t_D) = \frac{4}{3}((1+\Delta t_D)^{1.5} - \Delta t_D{}^{1.5})$, $g_o = \frac{4}{3}$ and $\Delta t_D = \frac{t - t_p}{t_p}$ for α=1 (low leak-off) Eq. (2)

Where $g(\Delta t_D) = (1+\Delta t_D) sin^{-1}((1+\Delta t_D)^{-0.5}) + \Delta t_D{}^{0.5}$, $g_o = \frac{4}{3}$ and $\Delta t_D = \frac{t - t_p}{t_p}$ for α=0.5 (high leak-off). Eq. (3)

The G time is calculated using pumping time and shut-in time, and it is used to analyze changes in leak-off pressure over time by calculating dP/dG and GdP/dG. The downward deviation from the linear slope of GdP/dG versus G time marks the fracture closure, associated with a brief zero-slope period followed by a decline in dP/dG versus G time, as discussed by Castillo (1987)[16]. Nolte's initial technique was based on several assumptions about pumping and shut-in periods and a simplified concept of fracture propagation and closure. The basic assumptions for the technique's applicability include: the fracture maintains a constant height; propagates through a quasi-elastic formation with negligible slip of bedding planes; is created by a constant injection rate of a power-law fluid into two symmetric wings; propagates continuously during pumping and stops when pumping ceases; and closes freely without significant interference from proppant. These assumptions ensure that the model accurately reflects the fracture's behavior under specified conditions.

2.2. Tangent Method (Baree et. al. (2007)[18])

The primary difference between the tangent method and Nolte's (1979)[9] initial work lies in their mathematical manipulation of Nolte's original formulation. Deviation from ideal behavior can lead to misinterpretations of GdP/dG versus G time for fracture closure. Nolte's model is based on an idealized hydraulic fracture within a linear-elastic, homogeneous medium of constant permeability. However, such ideal conditions are rarely encountered in real-world applications. If we applied Nolte's linear model for fracture closure detection of non-linear behavior to real field cases, deviations from linear behavior occur prematurely in non-ideal leak-off behavior, resulting in an overestimated fracture closure pressure that does not align with the mechanical earth model for the reservoir. Conversely, the tangent method often detects fracture closure at lower pressures due to the high net pressure caused by the injection of a small volume of fracturing fluid, typically a few thousand gallons, during DFIT.

To address the complexities of fracture closure, the tangent method was introduced as a modification to Nolte (1979)[9] . The tangent method proposed four types of leak-off during closure: normal leak-off (as seen in figure 2(a)), pressure-dependent leak-off (as seen in figure 2(b)), transverse storage leak-off (as seen in figure 2(c)), and tip extension leak off(as seen in figure 2(d)). It is derived from a plot of GdP/dG versus G, and closure pressure is defined as the pressure at which GdP/dG begins to deviate downward with a rule of thumb of the Gpd/dG cannot increase again after closure. The tangent method was developed to match numerical simulations by Barree and Mukherjee (1996)

 doi:10.20944/preprints202408.0725.v1

[17] and Barree et al. (2009) [19] and can reveal reservoir properties such as the presence of natural fractures, lower permeability streaks, or weak barriers around the pay zone. The log-log and the square root of time methods can be combined as the "Holistic Fracture Diagnostics" as described by Baree et. al. (2007)[18]. To achieve a reliable analysis, it is required to account for deviations from these ideal assumptions and to explore the impact of realistic conditions, including the complexities of wellbore and reservoir environments.

Baree et. al. (2016)[32] investigated the non-linear pressure-time derivative behaviors observed in diagnostic fracture injection tests (DFITs). While previous studies have predominantly used mathematical theories and conventional pressure transient theory to explain these behaviors, they often fail to consider the physical processes driving the observed pressure responses. They provided a clearer understanding of the mechanical and physical processes occurring during fracture extension and closure in DFITs, highlighting two primary sources of non-linear leak-off behavior: accelerated leak-off and delayed leak-off.

The ideal linear leak-off scenario assumes a formation that behaves as a perfectly linear-elastic, isotropic, and homogeneous medium with constant permeability, pore pressure, and closure stress. The fracture is expected to conform to the Perkins-Kern-Nordgren (PKN) or Khristianovitch-Zheltov-Geertsma-de Klerk (KGD) models, maintaining constant height, area, leak-off coefficient, and compliance. Under these ideal conditions, pressure decay follows a predictable linear model, resulting in straight lines on the G-function derivative analysis plot. However, real-world conditions often deviate from this ideal behavior, leading to non-linear leakoff responses. Accelerated leak-off is one such deviation, which can be influenced by wellbore effects and reservoir and fracture geometry effects. In terms of wellbore effects, decompression of fluid in the wellbore can cause an initial rapid pressure decline. Factors such as high near-well friction, and inefficient perforations. Tortuosity, either near the wellbore or far-field, contributes to this behavior. For instance, in horizontal wells, near-well fractures can create significant pressure drops, causing the observed instantaneous shut-in pressure (ISIP) to misrepresent the actual fracture extension pressure.

Reservoir and fracture geometry effects also play a crucial role in accelerated leakoff. The presence of shear fractures can increase the system's effective modulus, leading to an accelerated pressure decline. This behavior may indicate a complex fracture network or enhanced permeability regions. For example, in formations with open natural fractures, the hydraulic fracture aperture can close surrounding fractures, increasing the bulk system modulus and causing a faster pressure decline.

Delayed leakoff, another deviation from the ideal model, is often more problematic than accelerated leak-off. Wellbore effects such as the presence of highly compressible wellbores, including those with trapped gas pockets, can slow the pressure decline. Deformation and rebound of external packer elements or pipe contraction can also add energy to the system, reducing the rate of pressure decline. Reservoir and fracture geometry effects significantly impact delayed leak-off.

In horizontal wells, the formation of multiple fractures, such as longitudinal and transverse fractures, can store fluid and delay pressure decline. Longitudinal fractures, which open against higher normal stress than transverse fractures, close first and transmit higher pressure to transverse fractures, delaying their closure. The paper discusses how this interaction between fractures can lead to delayed leak-off signatures in the pressure-time data.

The concept of exponential leak-off describes a constant exponential pressure decline, often observed in low permeability reservoirs such as coal and shale formations. This behavior indicates pressure loss along a low conductivity fracture with minimal fluid loss to the surrounding rock mass. The G-function characteristics derived from this behavior show non-linear pressure and derivative responses, reflecting the complex interactions within the fracture and surrounding rock mass.

The discussion emphasizes the importance of understanding the physical mechanisms behind non-ideal pressure decline behaviors. Accelerated leak-off can result from wellbore decompression and after flow, as well as changes in reservoir properties such as increased permeability and modulus. Delayed leak-off may be influenced by complex fracture geometries, multiple fractures, and changes

 doi:10.20944/preprints202408.0725.v1

in pore pressure. The study highlights the need to consider these physical processes when interpreting pressure decline data to avoid misinterpretations.

Accurate interpretation of pressure decline behaviors requires an understanding of the physical mechanisms at play, including wellbore effects, reservoir properties, and fracture mechanics. The interaction of these multiple mechanisms can make interpretation ambiguous without additional information about the well, completion geometry, and reservoir properties. Analytical models must incorporate realistic conditions to provide valuable insights for fracture characterization and stimulation treatment design.

Based on the tangent method, The G-Function plots provide insightful details on fracture closure pressures across four distinct leak-off types in rock matrices. The Normal Leak-off type is characterized by a constant fracture area during shut-in, with fluid leaking uniformly through a homogenous rock matrix. This leak-off behavior is typically identified on the G-Function curve by a constant pressure derivative (dP/dG) and a linear G-Function derivative (G dP/dG) that passes through the origin. A deviation from this linearity indicates the fracture closure point, marked by a specific time and pressure. On the other hand, Pressure-Dependent Leak off (PDL) indicates the presence of secondary fractures that intersect the main fracture, distinguished by a noticeable "hump" in the G-Function derivative lying above the straight line from normal leak-off data. This hump signifies an increased leak-off rate due to a larger exposed surface area. After this peak, the pressure returns to normal leak-off behavior, with the hump's end marking the "fissure opening pressure." Transverse Storage / Fracture Height Recession and Fracture Tip Extension types also exhibit distinct patterns. The former shows a slower-than-normal leak-off due to intercepting secondary fractures that provide pressure support, while the latter features a fracture continuing to grow post-injection in low-permeability reservoirs, identified by a concave-down curvature in the G-Function derivative. These nuanced behaviors underscore the complex dynamics of fluid leak-off in fractured rock systems.

Using G function is conventionally used with the square root of time and the log-log technique as a confirmation for the closure pressure detected using GdP/dG vs. G time plot. A square root plot is a common method for determining closure pressure. When plotting the square root of time (x-axis) against the bottom-hole pressure (y-axis), the linear portion of the plot will align with a straight line passing through the origin. The point where the plot deviates from this straight line on the superposition plot (second derivative) indicates the closure pressure. Every square root plot typically features three main curves: the pressure curve, the first derivative, and the second derivative (also called the superposition curve). The minimum closure pressure is identified when the pressure curve deviates from the straight line, while fracture closure is pinpointed where the second derivative curve deviates from the line through the origin.

 doi:10.20944/preprints202408.0725.v1

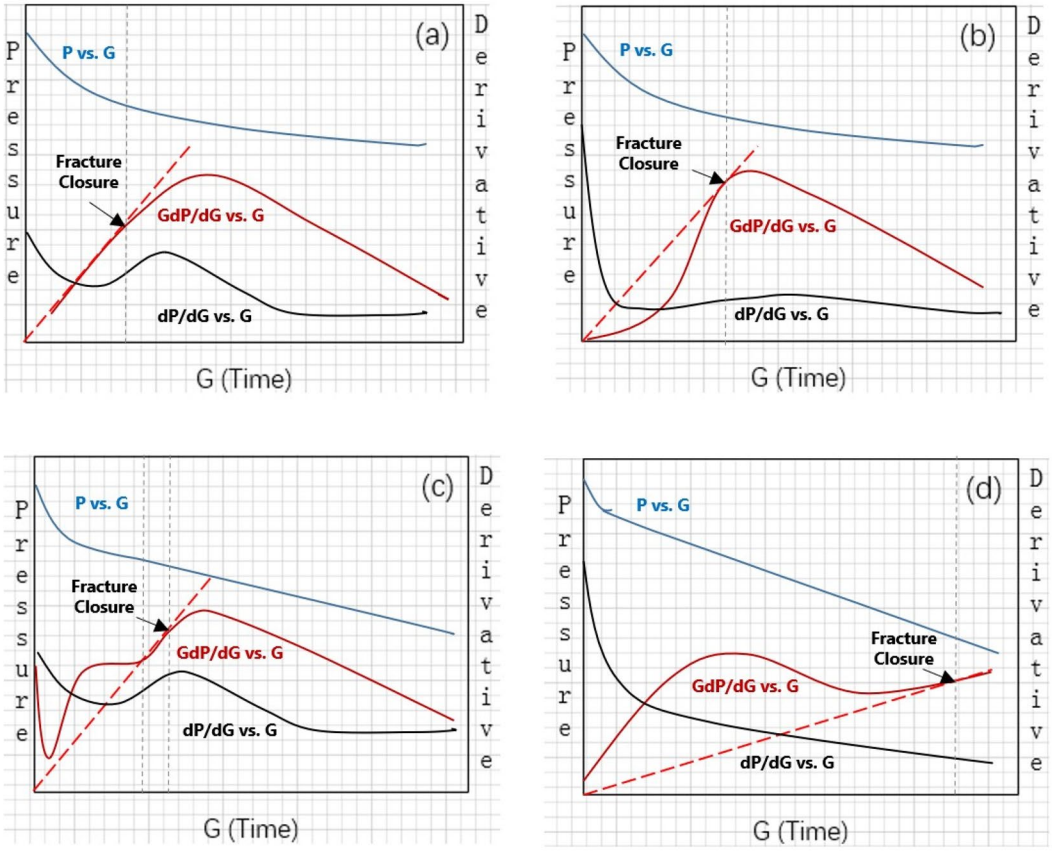

Figure 2. Type of pressure behavior vs. G-function, dP/dG vs. G-function, and GdP/dG vs. G-function trends: (a) normal leak-off behavior and (b) non-ideal leak-off behavior (I) that depicts a signature of height recession/transverse storage. (c) Non-ideal leak-off behavior (II) depicts a signature of pressure-dependent leak-off behavior, which occurs when the fluid-loss rate varies significantly with the pressure-dependent permeability in a dual-porosity system (usually micro-cracks and natural fractures exist in these cases). (d) Non-ideal leak-off behavior (III) that demonstrates a signature of fracture tip extension, which occurs in low-permeability reservoirs. (Liao et. al. (2022)[33]).

High net pressure in hydraulic fracturing jobs can be attributed to several interconnected factors discussed Han et. al. (2019) [34]. Primarily, rock laminations with lower permeability and weaker structural integrity can significantly increase net pressures due to poor energy dissipation across the formation. Additionally, the design and orientation of perforations are crucial; dense or complex patterns can lead to stress perturbations and interference between neighboring fractures, necessitating higher pressures for effective fracture propagation. The alignment of the wellbore relative to the natural in-situ stress directions also plays a critical role; misalignments can increase the resistance against fracturing, thus elevating required pressures. Furthermore, geological discontinuities such as natural fractures or faults can alter fracture paths, potentially arresting or diverting fractures and increasing the pressures needed to bypass or penetrate these barriers. Lastly, inefficient perforation designs that fail to adequately penetrate the formation or that are irregularly spaced can create uneven stress fields and increase frictional losses, thereby raising the net pressure. Ignoring all these factors we can observe up to 5,000 or 6,000 psi of net pressure because it includes all these friction losses. Another reason why the tangent method gives a lower estimate of fracture closure is the effect of post-closure reservoir fluid flow behavior as will be proven in our reverse engineering approach.

From a square root plot, a log-log plot (ΔP vs. shut-in time) is derived, providing a detailed means of identifying closure and various flow regimes before and after closure. The second derivative of the log-log plot reveals different flow regimes. Before closure, the half-slope line (1/2 slope) indicates a linear flow regime, while the quarter-slope line (1/4 slope) corresponds to a bilinear flow

 doi:10.20944/preprints202408.0725.v1

regime. After closure, a negative half-slope line (-1/2) signifies a linear flow regime, a negative three-fourth slope (-3/4) represents a bilinear flow regime, and a negative unit slope (-1) indicates a pseudo-radial flow regime. The equations (4) and (5) elucidate the mathematical relationships underpinning these analyses, demonstrating how bottom-hole pressure (P), Instantaneous Shut-in Pressure (ISIP), and the change in pressure (ΔP) can be plotted and interpreted through logarithmic transformations to reveal these key flow characteristics.

$$m(\sqrt{t}) = P - ISIP = \Delta P \tag{4}$$

Where t is the shut-in time and m is the slope of pressure vs. square root of time plot. Then by applying log to both sides, produces equation (5).

$$\log \Delta P = \log(m) + 0.5 \log(t) \tag{5}$$

Equation (5) proves that square root time is one flow regime identification for using a log-log plot (ΔP vs. shut-in time).

Barree et. al. (2007)[18] introduced a detailed review of the mathematical background of the log-log plot of pressure change with shut-in time as a technique to identify different flow regimes which are pre-closure linear, pre-closure bilinear flow, post-closure bilinear, post-closure pseudo-linear, post-closure pseudo radial flow regime. Table 1 shows the characteristic slopes of different log-log graphs. $t\partial\Delta p_{wf}/\partial t$ vs. t on a log-log plot is selected in our study for the reverse engineering approach to validate the effect of flow regime changes on the tangent and compliance methods approaches.

Table 1. the characteristic slopes of different log-log graphs.

Log-log	**Before Closure**		**After Closure**		
	Bilinear	Linear	Bilinear	Pseudolinear	Pseudo-radial
Δp_{wf} vs. t Δp_{awf} vs. t_a	¼	1/2	--	--	--
$\partial\Delta p_{wf}/\partial t$ vs. t $\partial\Delta p_{awf}/\partial t_a$ vs. t_a	-3/4	-1/2	-7/4	-3/2	-2
$t\partial\Delta p_{wf}/\partial t$ vs. t $t_a\partial\Delta p_{awf}/\partial t_a$ vs. t_a	1/4	1/2	-3/4	-1/2	-1
$t^2\partial\Delta p_{wf}/\partial t$ vs. t $t_a^2\partial\Delta p_{awf}/\partial t_a$ vs. t_a	5/4	3/2	1/4	1/2	0

McClure et al. (2014)[35] concluded that log-log superposition-time derivative plots can be used to diagnose flow regimes in DFIT transients, but interpreters must be aware that using superposition time causes the plot to curve upward when shut-in time equals injection time. The G-function experiences a downward bend at the same time, reflecting a decrease in slope of 1/2, while the superposition-time bend causes an increase in slope of unity. Understanding the complex relationship between the curve's slope and the scaling of pressure with time is crucial, as there is no physical significance to the 3/2 slope on the plot. To avoid confusion, McClure et al. (2014) [35] recommend interpreting DFIT transients from the basic pressure-transient interpretation plot—the log-log plot with the derivative taken with respect to actual time. To assist in identifying closure and other pre-closure trends, plots of pressure and GdP/dG vs. G can be used.

2.3. Compliance Method (McClure et al. (2014[20], 2016[21]))

The compliance method, introduced by McClure et al. (2014[20], 2016[21]) and Jung et al. (2016), provides earlier and higher stress estimates compared to the tangent method developed from the Nolte (1979)[9] technique and later modified by Barree et al. (2009)[19]. This method focuses on contact pressure rather than closure pressure and utilizes detailed DFIT simulations to consider the residual fracture aperture after the wall contact.

These simulations indicate that in low permeability formations, contact between fracture walls increases the pressure derivative, a signal previously interpreted as height recession or transverse

 doi:10.20944/preprints202408.0725.v1

fracture closure. The underlying mechanics of the compliance method derive from geomechanics principles concerning fracture closure. As noted by Sneddon (1946)[36], contact between fracture walls increases system stiffness and decreases the storage coefficient, leading to a rise in the magnitude of dP/dG. This method plots the magnitude of dP/dG, identifying the point where it begins to increase after reaching a minimum, suggesting a closure pressure 75 psi lower than the contact pressure.

This method aligns with classical approaches but also considers that an upward deflection in dP/dG may not always be present during shut-in transients, possibly due to rapid closure from near-wellbore tortuosity or continued fracture propagation. The changes in system stiffness before and after wall contact are crucial for estimating the minimum horizontal stress (Shmin). Analytical models like radial and PKN crack models determine system stiffness prior to fracture wall contact. After wall contact, increased stiffness results from the stress exerted by the contacting walls, as detailed by McClure et al. (2016) [21].The contact stiffness is mathematically represented as seen in Eq. (6):

$$S_{fc} = \frac{E'}{1-v^2}\frac{W_0^2}{12(1-v)} \tag{6}$$

where W0 denotes the aperture at contact, and E′ and ν are the effective Young's modulus and Poisson's ratio, respectively. This model assumes a specific form of the aperture relation, drawing from the works of Barton et al. (1985)[37] and further refined by Willis-Richards et al. (1996)[38]. The compliance method for stress estimation is based on mathematical solutions of the fracture closure process (McClure et al., 2016[21]). McClure et al. (2016[21], 2019[39]) provide the mathematical basis for the compliance method, with Equation (7) defining the relationship:

$$\frac{dP}{dG} = \frac{1}{C_t}\frac{dV}{dG} \tag{7}$$

where P is pressure, G is G-time, Ct is the storage coefficient, and V is the fluid volume in the system. The storage coefficient measures the volume of fluid released per unit pressure drop, influenced by fluid density and system volume changes.

Early in the shut-in phase, the early period is generally ignored due to rapid pressure drops. Subsequently, the pressure versus G-time plot shows a linear section that is extrapolated back to the y-axes intercept to estimate the far-field fracture pressure at shut-in, known as the effective initial shut-in pressure (ISIP). Once this initial phase passes, the pressure curve stabilizes into a nearly straight line. When the fracture walls make contact, an increase in stiffness results in a rise in dP/dG, marking the point used for stress estimation in the compliance method. This method, adjusting for stress shadow by subtracting 75 psi from the contact pressure, is informed by simulation matches to field DFITs, as described by McClure et al. (2019)[39].

Estimating the minimum horizontal stress (Shmin) involves analyzing changes in system stiffness and pressure transient behavior during and after fracture contacts. Numerical simulations that reflect field data suggest that the contact pick typically occurs around 75 psi above Shmin, as observed in figures 3(a) and 3(b). Nevertheless, uncertainties due to the roughness and heterogeneity of actual fractures compared to models can alter predictions, suggesting a potential error margin of 100-200 psi when estimating Shmin. The assumption that the fracture does not propagate after shut-in underpins the G-function; however, this may not always hold true. The presence of near-wellbore tortuosity can sometimes render stress estimates uninterpretable. Analysis by McClure et al. (2022)[40] indicated that 59% of cases showed a clear upward deflection in dP/dG, 25% showed an adequate deflection, and 16% showed no upward deflection.

 doi:10.20944/preprints202408.0725.v1

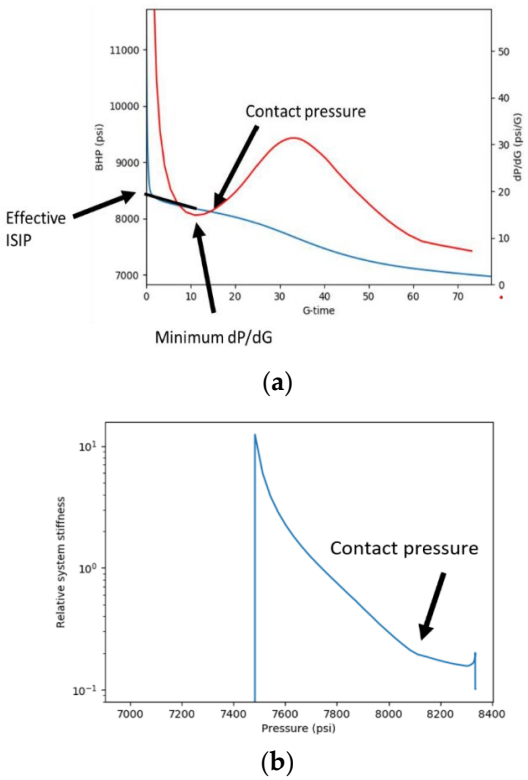

Figure 3. Example of compliance method (a) Shut-in pressure and dP/dG vs. G time (b) Relative system stiffness vs. shut-in pressure (Guglielmi et al. (2022) [56]).

2.4. Variable Compliance Method

The new model presented by Wang and Sharma (2017)[23] addresses the limitations of the G-function model by incorporating the gradual changes in fracture stiffness and pressure-dependent leak-off. This approach recognizes that fracture closure is a progressive process, starting at the edges and moving towards the center as pressure declines. The model integrates unsteady-state reservoir flow behavior, elastic fracture mechanics, and material balance to provide a comprehensive analysis of DFIT data.

This study includes synthetic cases and field data to demonstrate the coupled effects of fracture geometry, fracture surface asperities, formation properties, pore pressure, and wellbore storage on fracturing pressure decline and the estimation of minimum in-situ stress. The results show that traditional "normal leak-off" behavior, modeled using Carter's leak-off, is an oversimplification that leads to significant interpretation errors. The new model reveals that previous methods often overestimate or underestimate minimum in-situ stress due to their failure to account for changes in fracture compliance during closure.

Fracture compliance changes continuously as the fracture closes on rough surfaces and asperities, contrary to the assumption of constant compliance in traditional models. This variability significantly impacts pressure decline trends and the interpretation of DFIT data. The study proposes a "variable compliance method" to estimate minimum in-situ stress more accurately, which averages the G-time or square root of time of traditional and compliance methods.

2.5. Continuous Wavelet Transform Technique

Wavelet analysis was first introduced to the oil industry by Soliman et al. (2003)[41], specifically for well-test analysis and fracturing applications[42][43]. Ebru et. al. (2019)[44] introduced an innovative methodology for detecting fracture closure pressure using Discrete Wavelet Transform (DWT). This technique identifies closure pressure by analyzing detail levels to pinpoint changes in variance. Building on this, Eltaleb et al. (2020)[45] introduced a rigorous approach employing wavelet transform and energy density plots to represent noise energy in recorded pressure across various

 doi:10.20944/preprints202408.0725.v1

frequency levels. This method determines closure pressure by identifying the point where energy noise in the recorded pressure reaches its minimum level. This approach was further validated through a case study on the Utah FORGE formation, demonstrating its effectiveness in analyzing fracture injection tests in geothermal reservoirs (Eltaleb et al., (2021)[46])

Gabry et. al. (2023a)[47] introduced the continuous wavelet transform fracture closure detection technique and validated it using planar 3D fracture simulation, flow regime modeling and cross-validation with other techniques. In their technique, the first step is to apply the continuous wavelet transform (CWT) using a complex Morlet wavelet to the pressure signal as per equation (8) and equation (9), starting from the shutdown of the DFIT pumping.

This operation yields the CWT coefficients at different scales up to (a = 256). Subsequently, the wavelet transform modulus (WTM) is computed as per equation (10) from the complex continuous wavelet coefficients then calculating the signal energy as per equation (11).

$$T(a,b) = \frac{1}{\sqrt{a}} \int_{\infty}^{\infty} x(t)\psi^*(\frac{t-a}{b})dt \tag{8}$$

$$\psi^*(t) = \frac{1}{\pi^{1/4}} e^{i2\pi f_0 t} e^{-t^2/2} \tag{9}$$

Where f_0 represents the central frequency of the wavelet. f_0 equals to 1 for this application.

$$T(a,b) = \sqrt{[\mathrm{Im}(T(a,b))]^2 + [\mathrm{Re}(T(a,b))]^2} \tag{10}$$

$$E(a,b) = |T(a,b)| \tag{11}$$

Equation (6) comprises both the signal x (t), which could represent the pressure leak off time series signal, the mother wavelet function $\psi^*(\frac{t-a}{b})$ at a specific scale (a), and location (b). T (a, b) is the wavelet transform modulus at a specific scale (a) and location (b) with the imaginary part being Im(T(a,b) and the real part being Re(T(a,b). E (a, b) is signal energy at a specific scale (a) and location (b).

Considering that fracture closure is a dominant feature, it can be detected by averaging the logarithm of signal energy values at each time point for different scales (up to scale (a) = 256). From the plotted signal average log2 energy versus time, the start and the end of the fracture closure event can be identified with the following characteristics;

The start of the fracture closure, which represents the contact of the two fracture faces, can be recognized by a peak in the average signal log energy at the onset of fracture closure. The fracture closure itself can be identified by the drop in the signal average log energy level to a minimum stabilized level. The start of this minimum stabilized level characterizes the end of the fracture closure process as seen in example discussed by Gabry et. al. (2023b)[48] shown in figure 4.

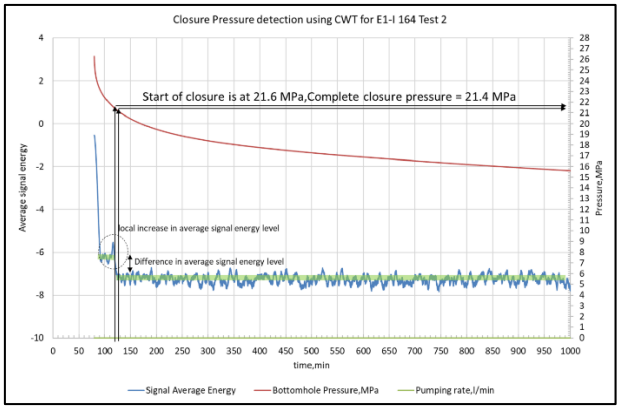

Figure 4. an example for fracture closure pressure detection using CWT fracture closure detection technique (Gabry et.al. (2023b)[48]).

 doi:10.20944/preprints202408.0725.v1

2.6. Other Techniques

Craig et al. (2014)[49] used type curve matching, known as the "Type Curve Method," to interpret closure and post-closure reservoir parameters. This technique operates on the principle that fracture closure is a storage phenomenon, incorporating both wellbore and hydraulic fracture components. By matching type curves, the method allows for a comprehensive analysis of the closure process and the subsequent behavior of the reservoir, providing valuable insights into the underlying dynamics.

Liu and Ehlig-Economides (2015)[50] utilize a combination of analytical and semi-analytical models to match pressure histories, specifically addressing "abnormal" pre-closure leak-off behaviors. These behaviors include tip extension, pressure-dependent leak-off, transverse storage, and multiple (vertical) closures, collectively referred to as the "Multiple Closure Method." This approach enables a detailed understanding of complex leak-off mechanisms that occur before the fracture fully closes, enhancing the interpretation of fracture behavior and improving the accuracy of reservoir parameter estimation.

Hoek (2016)[51] presents an analytical solution based on 3-D fracture simulation for water injector leak-off tests, which computes leak-off signatures given specific input geometry conditions. This approach distinguishes between storage-dominated cases, such as mini-fracture tests, and leak-off dominated scenarios, like water injection well pressure fall-off tests, referred to as the "Storage/Leak-off Bounded Method." Hoek emphasizes the superior results obtained in 'mid-leak-off' cases using this technique, showcasing its effectiveness in capturing the nuanced behavior of fracture leak-off processes.

Siddiqui et. al. (2017) [52] introduced a novel approach for analyzing diagnostic fracture injection fall-off tests (DFIT). This method diverges from traditional techniques by developing a model based on fundamental fluid flow and material balance equations, tailored specifically to the post-shut-in, pre-fracture closure period. Unlike the established Carter and Nordgren methods, which often do not account for field conditions adequately, this new model addresses fluid leak-off by considering the continuous nature of fluid flow in porous media, rather than discrete summation steps. However, it assumes constant stiffness. The analytical solution derived from this model, validated against field data, allows for the accurate estimation of fracture half-length and height product ($x_f \times h_f$) and closure pressure.

Zanganeh et al. (2017)[53] utilize numerical stress-pore pressure simulation to interpret pressure fall-off behavior, considering both leak-off and geometry changes, including after-flow effects that simultaneously narrow and extend the fracture length. This method, known as "Moving Hinge Closure," aims to capture the dynamic changes occurring during Diagnostic Fracture Injection Tests (DFITs). The authors integrate simplified elements of this interpretation into their model presented in the paper. However, a notable drawback of this approach is its reliance on numerical simulation, which may not be readily accessible for many engineers, thus limiting its widespread application.

3. Calibration Using Physical Measurements

3.1. Strain Gauges Measurements

Dutler et al. (2020)[54] utilized strain measurements to evaluate various fracture closure detection techniques, finding that the tangent method yielded the lowest minimum principal stress compared to other conventional methods. However, there are notable issues with their study. Primarily, the injection protocol did not adhere to the main assumptions of the G-function, which requires a constant injection rate for an extended period. Instead, the tests were conducted under constant pressure during the injection period. Additionally, Dutler et al.'s methodology for detecting closure pressure from the measured strain data did not follow the x-intercept rule proposed by Gulrajani and Nolte (2001)[55].

In a study by Guglielmi et al. (2022) [56], the 'tangent' and 'compliance' methods of interpreting fracture closure were compared against direct, in-situ strain measurements using the SIMFIP tool. The Step-Rate Injection Method for Fracture In-Situ Properties (SIMFIP) is equipped with a double packer hydrofracturing probe and a 6-component displacement sensor, installed within the sealed injection interval between two packers. As shown in Figure 5, the 2.41-meter-long injection interval

 doi:10.20944/preprints202408.0725.v1

houses a centrally positioned displacement sensor within a 0.24-meter-long and 0.1-meter-diameter pre-calibrated aluminum cage. This cage is linked to two 0.58-meter-long elements that facilitate clamping at the borehole wall, denoted as points A and B in Figure 5.

Upon clamping, the cage disconnects from the straddle packer system, allowing for the measurement of relative displacement between the upper and lower anchors, which are 1.4 meters apart. To qualify for inclusion in this study, the shut-in tests had to meet specific criteria: a minimum shut-in period of a few hours, SIMFIP measurements taken throughout the injection and shut-in phases, and assurance that the injection did not intersect or drain into a neighboring borehole. Four injection sequences from the Collab project that fulfilled these conditions were analyzed, although E1-I 164 Test 2 was included despite potential minor leakage into a grouted, neighboring observation well.

Figure 6 provides an example of a field test conducted using strain gauges to measure rock deformation as a physical detection method for fracture closure events. It also shows the numerical mechanical earth modeling and relative well locations of one of the test sites. The test sites conducted by the EGS Collab team include TV 4100 (7 tests) and E1-OT (3 tests).

The measurements were conducted during 2018 and 2019 across hydrofracturing experiments in boreholes drilled from the 4850' and 4100' levels of the mine, corresponding to approximately 1490.5 meters and 1250 meters below ground surface, respectively. The 69-meter-long E1-I borehole on the 4850 level slightly dips from horizontal, whereas the 50-meter-long TV 4100 borehole is vertical. Both boreholes penetrate fractured metamorphic rocks of the Sanford Underground Research Facility (SURF) in South Dakota, USA (Kneafsey et al., (2019)[57], (2020)[58]; Guglielmi et al., (2021)[59]).

The E1-I tests, referred to as the E1-I 164 Tests, and the TV 4100 tests, specifically TV 4100 Test 4 and TV 4100 Test 7, were conducted at various measured depths within these boreholes. Figure 6 also presents a 3D view of the injection borehole E1-I and the monitoring wellbore E1-OT for the E1-I 164 tests.

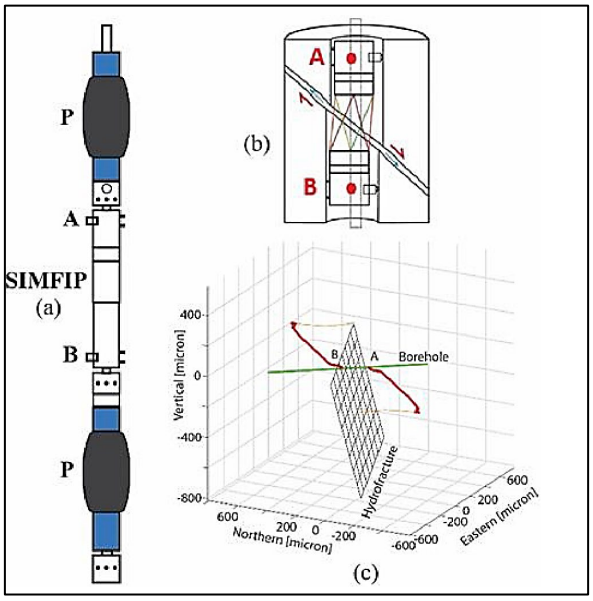

Figure 5. SIMFIP probe. (a) Design of the probe; (b) Schematic concept of the borehole three-dimensional relative displacement between anchors A and B ; (c) Example of a S IMFIP displacement signal captured across the activated hydrofracturing during E1-I 164 Test 2. Red segment is the displacement during injection and growth of the fracture. Orange segment is the displacement during shut-in. (Guglielmi et al. (2022)[56]).

 doi:10.20944/preprints202408.0725.v1

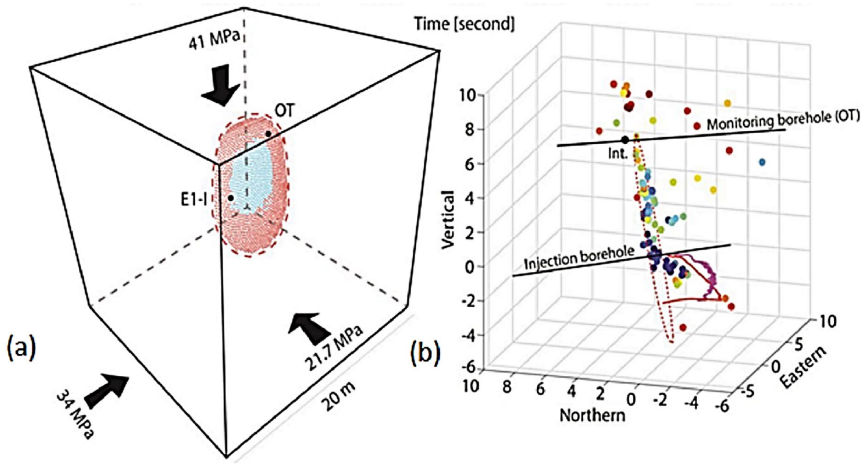

Figure 6. a) Numerical model setting with the calculated fracture at the end of the injection for E1-I164 Test (b) 3D view of the injection borehole E1-I and monitoring wellbore E1-OT (Guglielmi et al. (2020)[60]).

In the E1-I 164 tests, the vertical stress was estimated at approximately 41.8 MPa, with sub horizontal intermediate and minimum principal stresses (SHmax and Shmin) previously estimated at 34.0 MPa and approximately 21.7 MPa, respectively. These tests involved three propagation and shut-in steps, extending the fracture into the rock until intersecting a borehole 10 meters from the injection site.

Using continuous borehole displacement data from the SIMFIP probe, micro-shearing initiated on a foliation plane until the injection pressure exceeded 112% of the estimated Shmin, leading to the opening and sliding of a new hydro-fracture. The measured displacements and simple modeling indicated a mixed mode of fracture growth aligned with the ambient stress regime.

In the TV 4100 tests, eight SIMFIP tests monitored fracture displacement at different depths along the 50-meter-deep borehole to construct a stress profile and assess stress variability. These tests also explored other stress measurement techniques, such as conventional hydraulic and new thermal fracturing tests, some of which overlapped test intervals. The selected intervals for these tests were set in foliated amphibolite affected by cemented natural fractures, aiming to determine whether these fractures would activate under pressure or if new hydrofractures would form. Acoustic log comparisons before and after the tests did not reveal new fractures but indicated stronger acoustic contrasts along some segments of preexisting fractures, suggesting reactivation. These findings, along with the orientation of SIMFIP displacements, helped identify the most likely candidates for fracture reactivation and the mode of such reactivation.

A typical SIMFIP test involves several injection cycles. Initially, pressure is increased incrementally to a maximum that remains well below the fracturing pressure, then it is reduced to the starting level. This initial cycle is crucial for characterizing the hydromechanical response of the injection chamber, integrating the rock formation's mechanical response, the effects of mechanical coupling of the SIMFIP clamps and packers, and the probe's stiffness. A clear, though sometimes complex, correlation typically emerges between the borehole displacements and the pressure, with displacements reverting completely when the pressure returns to the initial level. Subsequent injection cycles aim to induce and expand fractures from the chamber away from the borehole. These cycles, whether constant flowrate or pressure step rate tests, also measure borehole displacements in addition to pressure and flowrate. At the fracturing pressure, the relationship between SIMFIP displacements and injection pressure changes, reflecting the orientation and activation mode of the newly created or reactivated fracture. Multiple cycles might be necessary to clarify the displacement orientation, especially in cases of local borehole tortuosity.

For instance, in the SURF E1-I 164 Test 1 at 1490.5 meters below ground surface (BGS), fracture nucleation started by shearing along a foliation plane at the borehole wall, strongly influencing early displacement measurements. Over time, as the injection continued, a significant macroscopic fracture

 doi:10.20944/preprints202408.0725.v1

developed and realigned perpendicular to the minimum principal stress, resulting in consistent displacement orientations noted in the subsequent E1-I 164 Test 2, indicating the reopening of the initial hydrofracturing. Various methods can be employed to estimate stress based on observed SIMFIP displacements and pressure. Ideally, the orientation of the SIMFIP displacement vector, when associated with the activation of a fracture, can be compared to the fracture geometry deduced from acoustic borehole wall logs conducted before and after the test.

In the E1-I 164 Tests 1 and 2, the geometry of the hydrofracturing was inferred from the alignment of seismic events and from distributed fiber optic temperature and strain data, pinpointing the fracture intersection with nearby monitoring boreholes. However, identifying activated fractures is less straightforward in the TV 4100 Tests 4 and 7, where natural fractures appear to have been reactivated. In these cases, the orientation of the SIMFIP displacements indicates whether the activated fracture lies between the anchors or outside them and is then compared to the mapped natural fractures seen on acoustic logs. Multiple natural fractures might be activated in these scenarios (Kakurina et al., 2020[61]).

The three-dimensional SIMFIP displacement data are subsequently decomposed into components tangential and normal to the activated fracture. The normal component, which manifests during fracture opening, directly correlates to the pressure at which this occurs, while the shear component can be used to augment the estimation of the stress tensor, perhaps through advanced techniques like Coulomb stress inversion (Guglielmi et al., 2020[59]). Section 9A from Gulrajani and Nolte (2001)[55] provides a methodology for estimating the magnitude of the minimum principal stress from deformation measurements, whether during shut-in or reopening. As depicted in Figure 6, the rock displacement should be plotted against pressure.

For a fracture perpendicular to the minimum principal stress, there exists a roughly linear relationship between deformation and pressure when the fracture is mechanically open but not propagating. If a preexisting fracture that is not perpendicular to Shmin reopens, the normal stress on the fracture exceeds Shmin, potentially leading to some irreversible shear as the fracture opens, especially if the fracture walls contain asperities that contact during closure, creating a back stress that nonlinearly increases stiffness. The intersection of the asperities at a width that is a fraction of the maximum width during injection demonstrates that if the fracture were perfectly smooth, this width would be zero, and the extrapolation line would stretch straight to zero on the x-axis in Figure 6. With a nonzero width, the curve deviates and curves asymptotically towards zero as pressure decreases below Shmin. The x-intercept of this straight line in Figure 7 is equal to Shmin, as shown in the diagram from Gulrajani and Nolte (2001) [55].

Identifying 'closure/reopening' might be tempting as the point where displacement visibly deviates from zero, but the gradual, asymptotic reduction in aperture continues even as pressure significantly drops below Shmin. Other complex hydromechanical phenomena also affect SIMFIP displacements, such as the fact that at the beginning of the first injection cycle into a section, the fracture has not yet formed, so the deformation versus pressure response cannot be used for stress analysis, and the mode of fracture activation often involves some irreversible shear-induced dilation rather than being purely tensile.

The SIMFIP tool was utilized to compare the tangent and compliance methods by Guglielmi et al. (2022) [56] and extensively investigated by Gabry et al. (2023b) [48], showing the results in Table 2. Gabry et al. (2023b) [48] explored the efficacy of the CWT closure detection technique and its correlation with closure pressures measured via rock displacement strain gauges using the SIMFIP tool. The study also uncovered that natural fractures attenuate the peak signal that typically indicates the initiation of fracture closure, resulting in a more gradual closure process.

This effect was observed as a smoother reduction in signal energy. They also established a linear relationship between closure time, as detected by the CWT technique, and the presence of natural fractures, highlighting the technique's sensitivity to natural fracture intensity. This relationship emphasizes the potential of the CWT method to adapt to and accurately reflect induced fracture complexity.

 doi:10.20944/preprints202408.0725.v1

It is noteworthy that the tangent method demonstrated significant improvement in performance with an increase in natural fracture intensity. This enhancement in accuracy was particularly evident in TV4100 Test 7, where the method achieved its highest level of precision. On the other hand, the compliance method exhibited a contrasting trend, showing a marked decline in accuracy as natural fracture intensity increased. The underlying reasons for these observed effects, including the factors contributing to the superior performance of the tangent method and the challenges faced by the compliance method under these specific conditions.

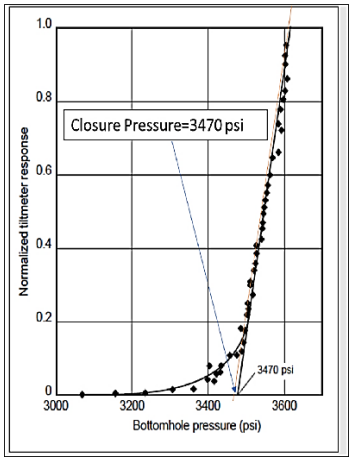

Figure 7. Schematic of hydraulic fracture reopening/closure. (Gulrajani and Nolte (2001)) [55].

Table 2. fracture closure detection results for EGS Collab data (Gabry et. al. (2023b)) [48].

	E1-I 164 Test 2	E1-I 164 Test 3	TV4100 Test 4	TV4100 Test 7
Fracture closure pressure using SIMFIP	**3100 psi**	**3100 psi**	**2712 psi-2785 psi**	**2700 psi**
Number of reported natural fractures	**0**	**Not reported**	**5**	**10**
fracture closure pressure using CWT fracture closure detection Technique	**Start of closure 3132 psi Complete closure 3103 psi**	**Start of closure 3000 psi Complete closure 2950 psi**	**Start of closure 2740 psi Complete closure 2700 psi**	**Start of closure 2760 psi Complete closure 2700 psi**
Fracture closure pressure using Compliance Method	**Rapid closure 3000 psi-3500 psi**	**2725 psi**	**2475 psi**	**2800 psi**
Fracture closure pressure using Tangent Method	**Less than 2200 psi**	**Less than 2200**	**Less than 2200 psi**	**2700 psi**
Fracture closure pressure using Nolte Technique	**3400 psi**	**No closure signature**	**2910 psi**	**3177 psi**
Fracture closure pressure using log-log method	**No closure signature**	**No closure signature**	**No closure signature**	**No closure signature**
Fracture closure pressure using the square root of time method	**No closure signature**	**No closure signature**	**No closure signature**	**2700 psi**

3.2. Fiber Optics Measurements.

Kerr et al. (2024)[62] conducted a field study at the Department of Energy's Austin Chalk/Eagle Ford Shale Laboratory (ACEFSL) to explore the application of Diagnostic Fracture Injection Tests (DFITs) using fiber optics monitoring. The study involved two consecutive DFITs on a well-

 doi:10.20944/preprints202408.0725.v1

instrumented with permanent fiber optics, followed by a larger DFIT that interacted with an adjacent observation well, also equipped with fiber optics.

The fiber optic data collected from both the treatment well and the offset observation well indicated a prolonged relaxation period following the cessation of injection. This relaxation, aligning with the diminishing fracture aperture during the "closure" process, persisted over several hours. The sustained relaxation is likely attributable to fluid recharge from longitudinal fractures into transverse fractures, driven by the anisotropic nature of the earth's stress tensor. Interpretations of fiber strain data suggest that fracture closure occurs uniformly and simultaneously throughout the entire fracture volume, rather than starting at the tips and progressing inward. At the treatment well, the compressive strain on the fiber was concentrated around the perforation areas, where the dominant transverse fractures were undergoing closure. During this relaxation and closure phase, no evidence of asperity contact was observed.

Further analysis using the derivative of the G-function, combined with modeling, confirmed that the timing of fracture "closure" corresponded with the extended relaxation signatures recorded by the fiber optics during multiple DFIT stages. The models demonstrated that after the cessation of injection, a recharge period ensued, where fractures opening against higher stresses maintained the observed wellbore pressure, thus delaying the full closure of the fractures. This study underscores the value of integrating fiber optics with DFITs for a more detailed understanding of fracture behavior and closure dynamics.

4. Field Scale Studies

Zanganah et al. (2018)[63] investigated the unique challenges posed by low leak-off formations during DFITs using the Duvernay Formation as a case study. This research addressed the complications in interpreting traditional DFIT data due to the unique geological and geomechanical conditions of the Duvernay shale. The researchers employed a sophisticated approach that integrated geological data, geomechanical simulations, and actual DFIT results. Their methodology involved evaluating DFIT data using traditional and newly developed pressure transient analysis methods. They created synthetic DFIT responses through two simulation models to match and explain the actual field data, focusing particularly on the phenomena of moving-hinge closure with tip extension and the activation of secondary natural fractures.

The study revealed that DFIT responses in the Duvernay shale are heavily influenced by low matrix permeability and the presence of a complex natural fracture network. This setting leads to significant tip extensions and episodic fracture growth, which traditional DFIT analysis methods fail to accurately capture. The pressure falloff during the tests is governed more by pressure dissipation through primary and secondary fracture networks than by fluid leak-off into the matrix, challenging conventional interpretations of closure pressures and formation permeability. The paper concluded that conventional DFIT analysis methods are inadequate for low leak-off formations like the Duvernay shale due to their inability to account for complex fracture dynamics and the minimal leak-off characteristic of these formations. The authors highlighted the need for revised DFIT interpretation methodologies that consider these unique challenges to avoid significant errors in estimating key reservoir and fracture properties.

Buijs (2021)[64] conducted a multi-basin analysis encompassing data from regions such as the North Sea, Europe, Russia, North Africa, and South America. This study integrated data from DFITs, core analyses, pressure build-up (PBU), rate transient analysis (RTA), and modern technologies like fiber optics and production logging tools (PLT). This wide-ranging data collection aimed to cross-validate traditional minimum stress interpretation techniques against newer methods, particularly those utilizing fracture compliance methodologies. Buijs discussed the implications of adopting different closure pressure estimation methods, emphasizing the potential risks associated with newer, less validated approaches. The discussion highlighted the importance of methodological rigor and the need to adhere to proven methods unless newer techniques provide clear, consistent, and replicable advantages. The study's results reinforced the reliability of traditional tangent method closure pressure estimation methods. These methods were substantiated through various case

 doi:10.20944/preprints202408.0725.v1

histories, comparing permeability estimates from different analysis techniques. The paper illustrated how newer methods could lead to discrepancies in fracture modeling and subsequent operational strategies, potentially hindering optimal hydraulic fracture processes.

5. Methodology

To comprehend fracture closure, an independent characteristic must be explored and modeled both prior to and following the closure. This characteristic is the fluid flow regime before and after closure. After the shut-in procedure, the pressure gradient along the fracture undergoes a brief period of linear flow due to pressure dissipation. In formations with low permeability and extended fractures, an initial linear flow phase may be followed by a bi-linear flow regime, where linear flow within the fracture coincides with linear flow from the reservoir. The duration of this reservoir's linear flow phase depends on the reservoir's permeability and the volume of fluid that has leaked from the fracture during closure.

Once the fracture closes, the pressure transient around the fracture propagates into the reservoir, transitioning to elliptical flow and eventually pseudo-radial flow. Each flow regime displays unique characteristics in various diagnostic plots. Figure 8 graphically represents these flow regimes before and after closure. Log-log plots of t dp/dt versus t help identify the different flow regimes and their corresponding slopes both before and after closure as per Table 1.

For pre-closure flow regimes, immediately after the pumps cease and the fracture begins to close, a short-lived one-dimensional linear flow occurs along the fracture's length. Both the Compliance method and the Tangent method utilize a common pre-closure analysis known as the G function, originally proposed by Nolte in 1979[9] and adapted over time. The Tangent method employs GdP/dG, while the Compliance method uses dP/dG to indicate stiffness during pressure leak-off.

Identifying flow regimes before and after fracture closure is crucial for analyzing real field data to determine pre-closure linear and bi-linear flows, and post-closure linear, bi-linear, and radial flows to estimate reservoir pressure and permeability accurately. However, pinpointing the start and end times of these periods is challenging due to factors like existing natural fractures, the stress state of the formation, and reservoir heterogeneity, which are often incompletely understood in many reservoirs.

A controlled, simplistic model is proposed to test each closure detection technique and assess their strengths and limitations. This involves reverse calculating the flow regime modeling on the log-log t dp/dt versus t diagnostic plot. This model can simulate all previous flow regimes and be reverse-engineered to generate time-series synthetic pressure data that follows pre-identified slopes for t dp/dt versus t over specified periods. This model can also examine the monotonic increase of the G function in the Tangent method and how natural fractures appear in the G function.

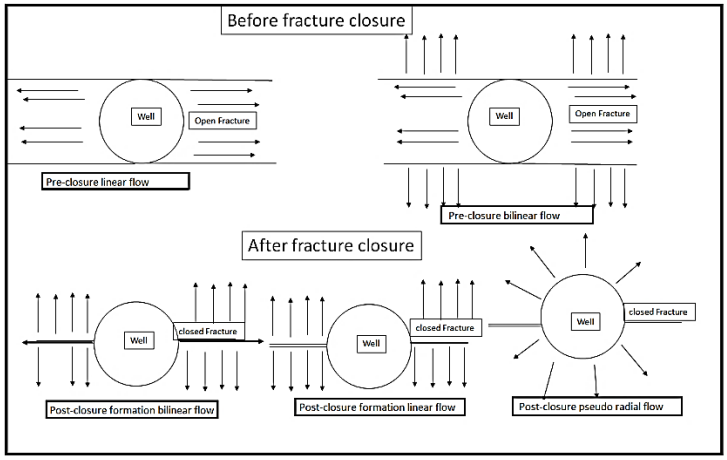

Figure 8. Transient flow regimes before and after fracture closure(Gabry et.al. (2023a)[47]).

 doi:10.20944/preprints202408.0725.v1

By using the equations for flow regimes before and after closure, a log-log diagnostic graph ($t\frac{dp}{dt}$ vs. t) can be generated to identify different flow regimes before and after closure as per 3rd row in table 1. The slope of log-log plot of ($t\frac{dp}{dt}$vs. t) can be used to identify the flow regime. If we assumed that slope to be with variable name (s) so we can get the equation (12) for number of n of pressure points.

$$s = \frac{\log(t_{i+1}\frac{dp_{i+1}}{dt_{i+1}}) - \log(t_i\frac{dp_i}{dt_i})}{\log(t_{i+1}) - \log(t_i)} \quad (12)$$

Where $dp_{i+1} = p_{i+1} - p_i, dp_i = p_i - p_{i-1}, dt_{i+1} = t_{i+1} - t_i, dt_i = t_i - t_{i-1}$and i =1, 2, 3… n.

Where (s) is 0.5 for pre-closure linear flow and 0.25 for pre-closure bilinear flow, -0.5 for post-closure linear flow, -0.75 for post-closure bilinear flow and -1 for post-closure pseudo radial flow. From this equation, we can calculate thep_{i+1} at any point using equation(13) by assuming the first pressure drop between the first two time points in the synthetic pressure drop.

$$p_{i+1} = p_i + \frac{t_{i+1} - t_i}{t_{i+1}} 10^{s\log\frac{t_{i+1}}{t_i} + \log t_i \frac{p_i - p_{i-1}}{t_i - t_{i-1}}} \quad (13)$$

The synthetic pressure signal is assumed to be 12,000 psi to allow adequate room for a reasonable leak-off in the signal. The parameter (α) is set to be 1 in G function calculations. An example of the pressure signal is shown in Figure 9. Table 3 shows the values of slopes of log-log t dp /dt versus t diagnostic plot used to create the pressure signal example in Figure 9.

Table 3. Slopes of log-log t dp /dt versus t diagnostic plot used to create the pressure signal example 1.

The Pumping period starts from 0 to 5 minutes (t_p = 5 min)			
Start time of priod (min)	End time of period (min)	Slope of log-log t dp /dt versus Δt diagnostic plot	Shut in period name
5	15	a = 0.75	Storage
15	40	b = 0.5	Pre-closure linear flow.
40	50	c = 0.25	Pre-closure bilinear flow.
50	70	d = -0.5	Post-closure formation linear flow.
70	200	e = -0.75	Post-closure formation bilinear flow.
200	400	f = -1	Post-closure radial flow.

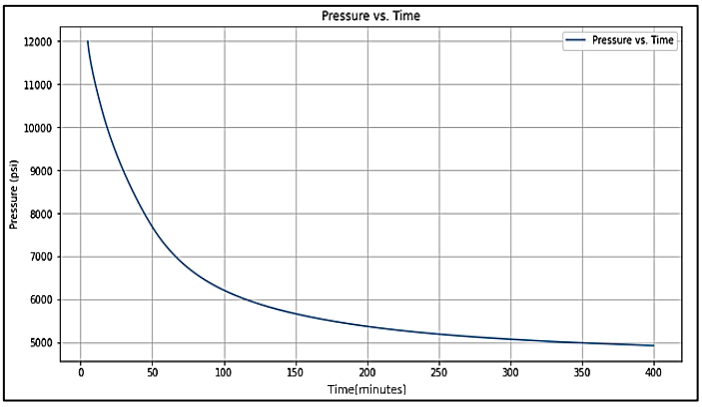

Figure 9. Example of the pressure signal example for slopes in table 3.

Our comparison methodology involves generating multiple shut-in pressure signals and then applying the tangent closure detection technique to evaluate the impact of flow regimes on fracture

 doi:10.20944/preprints202408.0725.v1

closure identification. This technique relies heavily on understanding flow regimes. Additionally, we will explore the core concept of the fracture compliance method, discussing its principles and delineating the boundaries of its applicability.

6. Results and Discussion

Changes in the slopes of different flow periods, treated as single-variable sensitivity while keeping the rest of the periods constant, can reveal how the GdP/dG is affected by each flow regime. This analysis helps to isolate the impact of individual flow periods on the overall pressure response.

The series of plots titled GdP/dG vs. G for different values of parameters (a) through (f), shown in Figures 10 through 15, provides a clear illustration of how each parameter distinctly influences the system's dynamics. These plots demonstrate the sensitivity of the GdP/dG curve to changes in specific flow regimes and highlight the importance of accurately characterizing these periods.

We can notice that disturbances in flow periods, specifically post-closure pseudo-linear flow (parameter e) and post-closure pseudo-radial flow (parameter f), severely affect the interpreted fracture closure pressure using the tangent method. The rule of thumb that GdP/dG shouldn't increase after closure no longer holds if these flow periods are disturbed. This disturbance can occur due to nearby well operations or in complex, dynamically disturbed natural fracturing systems. For instance, hydraulic fracturing activities in adjacent wells can alter the local stress field and fluid pressure distribution, leading to changes in the observed flow regimes. Similarly, natural fractures that are dynamically reactivated can also disrupt the expected flow patterns.

The tangent method relies on specific simplification models for the fracture closure process, which must be met to interpret the fracture closure pressure accurately. These simplifications assume a relatively stable and predictable flow regime following fracture closure. However, when these assumptions are violated—such as when post-closure flow regimes are disrupted—the accuracy of the tangent method in determining closure pressure is compromised.

The GdP/dG vs. G plots highlight how sensitive the interpreted fracture closure pressure is to changes in post-closure flow regimes. In an ideal scenario, the GdP/dG curve should show a clear trend that indicates fracture closure. However, disturbances in the flow periods can lead to anomalies in the curve, such as unexpected increases in GdP/dG after closure. These anomalies make it challenging to apply the tangent method correctly and can result in significant errors in estimating the closure pressure.

Therefore, it is crucial to carefully monitor and control the conditions during DFITs to ensure that the flow regimes remain stable and predictable. This involves considering the potential impacts of nearby well operations and natural fracture dynamics. Additionally, using complementary diagnostic techniques and integrating data from multiple sources can help to validate the interpreted results and provide a more robust understanding of the fracture closure process.

In summary, the series of GdP/dG vs. G plots demonstrates the importance of accurately characterizing flow periods in the interpretation of fracture closure pressure using the tangent method. Disturbances in post-closure flow regimes can significantly affect the results obtained using the tangent method, highlighting the need for careful monitoring and the use of complementary diagnostic approaches to ensure reliable interpretations.

Preprints.org (www.preprints.org) | NOT PEER-REVIEWED | Posted: 9 August 2024 doi:10.20944/preprints202408.0725.v1

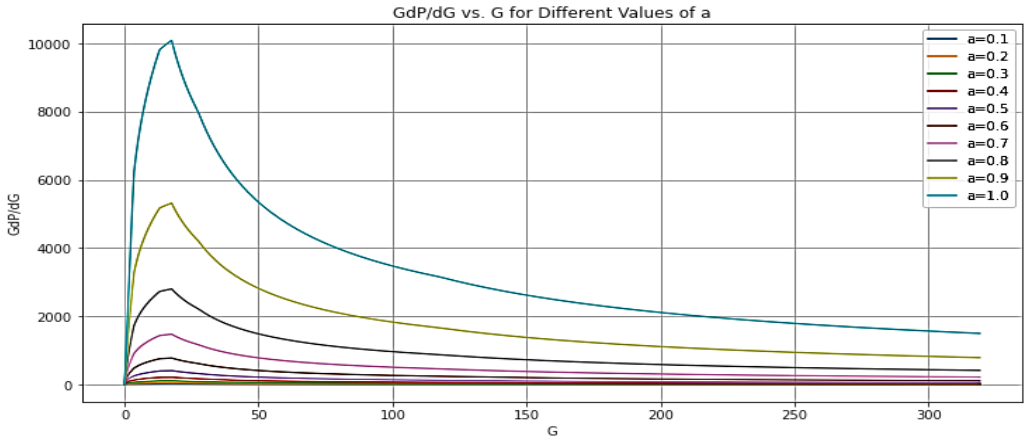

Figure 10. GdP/dG vs. G with disturbance in early flow period log-log slope.

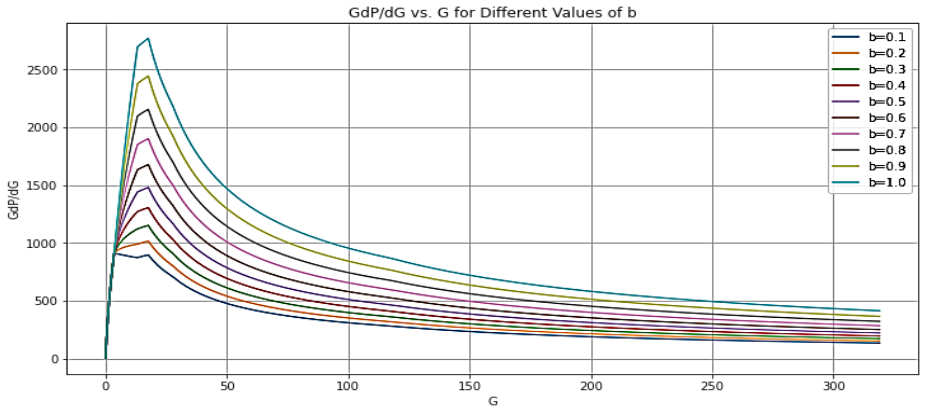

Figure 11. GdP/dG vs. G with disturbance in pre-closure linear flow log-log slope.

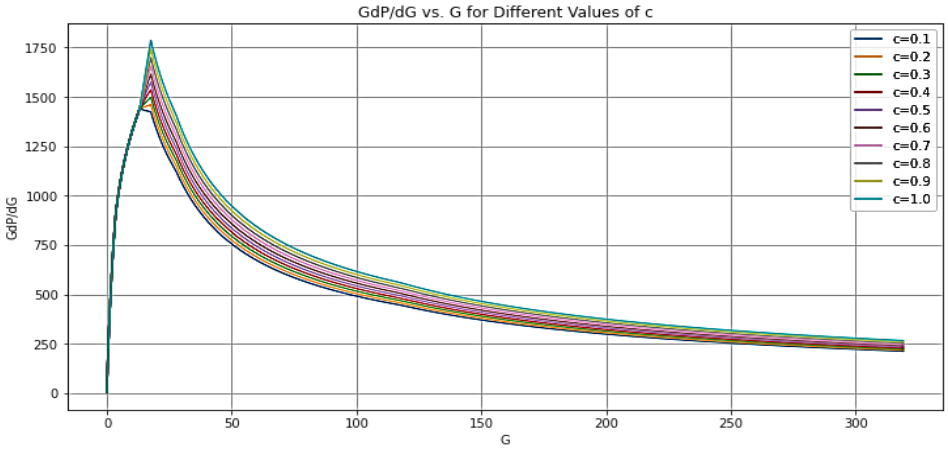

Figure 12. GdP/dG vs. G with disturbance in pre-closure bilinear flow period log log slope.

Preprints.org (www.preprints.org) | NOT PEER-REVIEWED | Posted: 9 August 2024 doi:10.20944/preprints202408.0725.v1

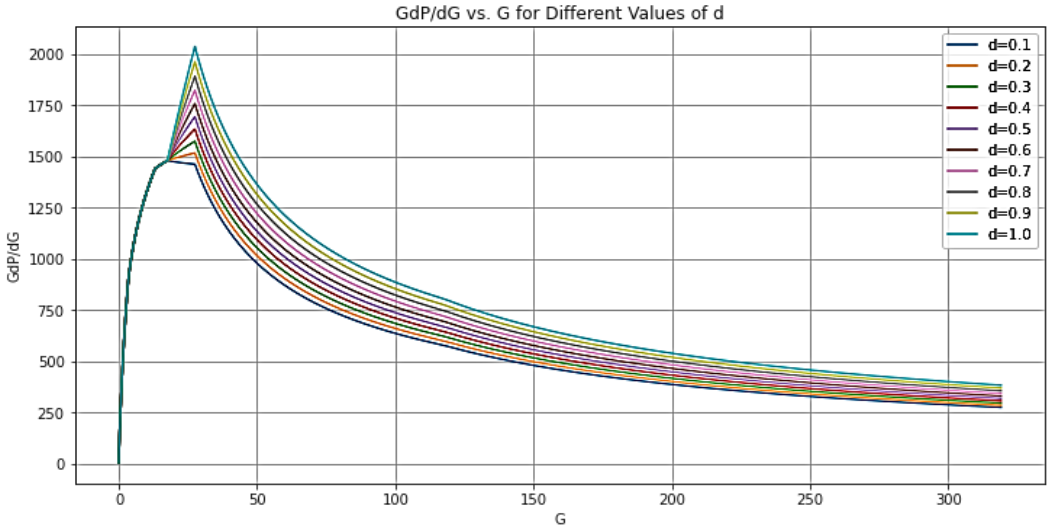

Figure 13. GdP/dG vs. G with disturbance in post-closure bi-linear flow period log-log slope.

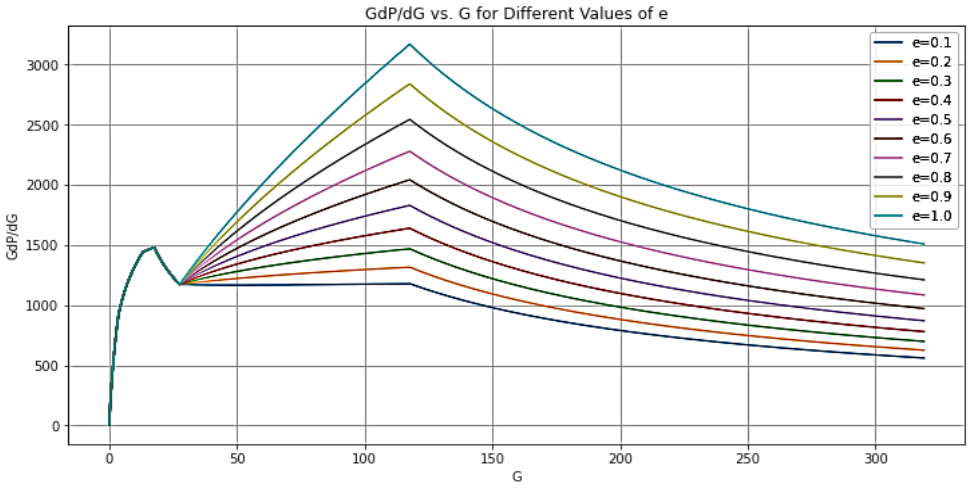

Figure 14. GdP/dG vs. G with disturbance in post-closure pseudo-linear flow log-log slope.

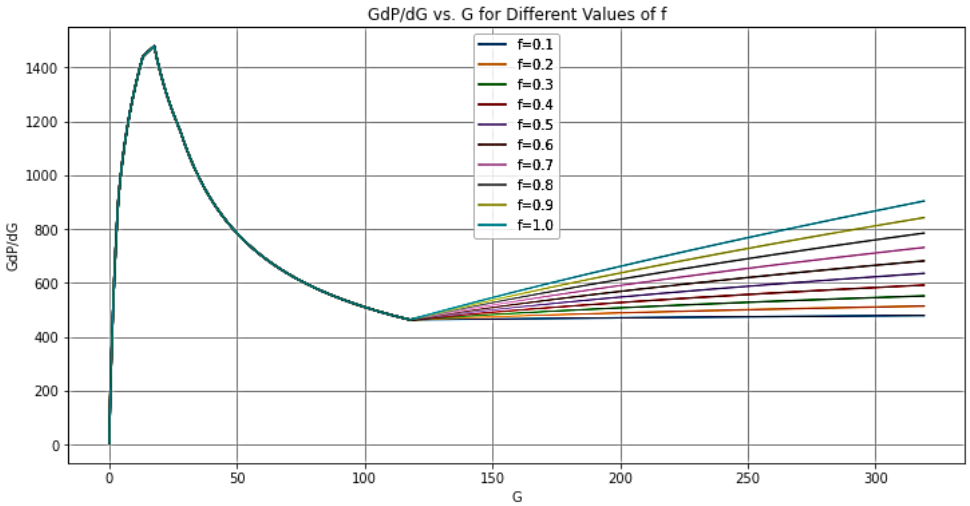

Figure 15. GdP/dG vs. G with disturbance in post-closure pseudo-radial flow period log-log slope.

On the other hand, fracture permeability significantly influences the total system stiffness in a reservoir, especially in the context of hydraulic fracturing. Fracture permeability refers to the ability

 doi:10.20944/preprints202408.0725.v1

of fractures within a rock formation to allow fluids to pass through them. System stiffness refers to the resistance of the reservoir rock and its fractures to deformation under stress, including both the rock matrix and the network of fractures.

Fractures are more compliant, or less stiff, compared to the intact rock matrix, and the presence of fractures generally reduces the overall system stiffness. High fracture permeability enhances fluid flow within the fractures. As fluid pressure within the fractures increases during hydraulic fracturing, it can lead to further opening of the fractures, reducing the stiffness of the rock mass. The permeability of fractures affects how stresses are redistributed around them. High permeability allows for quicker pressure equilibration, potentially leading to a more uniform stress field but lower system stiffness. In a network of fractures, the permeability of individual fractures influences their interaction. High permeability can lead to interconnected fracture networks, significantly reducing the overall system stiffness.

During the hydraulic fracture closure in low permeability compact reservoir rock with no natural fractures, it can be noticed that fracture closure is associated with an increase in system stiffness. If the rock itself is naturally fractured in equilibrium, the hydraulic fracture will not significantly reduce the system stiffness and it will not show an increase in system stiffness during the fracture closure process.

The compliance method concept is based on the increase in system stiffness during the fracture closure process. This increase in stiffness is not significantly observed in naturally fractured rock where natural fractures are initially in equilibrium. DFIT pumping disturbs this equilibrium, and during the shut-in period, the natural fracture system returns to its initial state with residual apertures, resulting in no significant increase in system stiffness. That is the reason of good results of compliance method in shale reservoirs with low natural fractures intensity. It worked well with formations that tend to propagate planar hydraulic fractures (low inducted fracture complexity). This hypothesis is supported by the lower percentage increase of dP/dG vs. G in naturally fractured reservoirs, such as the Canadian Montney Shale Play and Canadian Duvernay Shale Play.

Virues et al. (2023)[65] conducted a comprehensive comparative analysis of 80 diagnostic fracture injection tests (DFITs) from various operators in the Canadian Montney shale play. Their study aimed to refine DFIT interpretation best practices by examining two widely-used analytical methods: the "compliance" method by McClure et al. (2019)[39] and the "holistic" or tangent method by Barree et al. (2009)[19]. The pre-closure analysis (PCA) involved evaluating closure pressure, instantaneous shut-in pressure (ISIP), net fracture pressure, and leak-off behavior before fracture closure. For after-closure analysis (ACA), the authors used the Nolte and Soliman/Craig methods to analyze fall-off data and estimate permeability and reservoir pressure. A striking finding was that a clear "compliance" closure pressure signature was absent in 48% of the Montney DFITs analyzed. While the compliance and tangent methods produced similar closure pressure values (within an 8% difference on average), the clarity of the compliance closure response varied significantly across the dataset. Crucially, the estimated net fracture pressures differed substantially, with the tangent method yielding values approximately 10 times higher than the compliance method. This discrepancy has profound implications for fracture growth and production optimization. The authors demonstrated that the compliance method closure pressure signature is never associated with the PDL signature on the GdP/dG vs. G time plot over 80 DFIT cases in the Canadian Montney shale play. Instead, it is strongly correlated to the transverse fracture storage/fracture height recession signature on the GdP/dG vs. G time plot as seen in Figure 16.

This transverse fracture storage/fracture height recession is associated with shale or low leak-off formation within the main leak-off behavior, creating the hump in the GdP/dG vs. G time plot. This can occur at the edges of closing fracture geometry (fracture height recession) or lower leak-off shale lamina within the closing fracture geometry (transverse fracture storage). In both cases, the contribution of low leak-off zones (high permeability contrast) magnifies the stiffness change during fracture closure.

 doi:10.20944/preprints202408.0725.v1

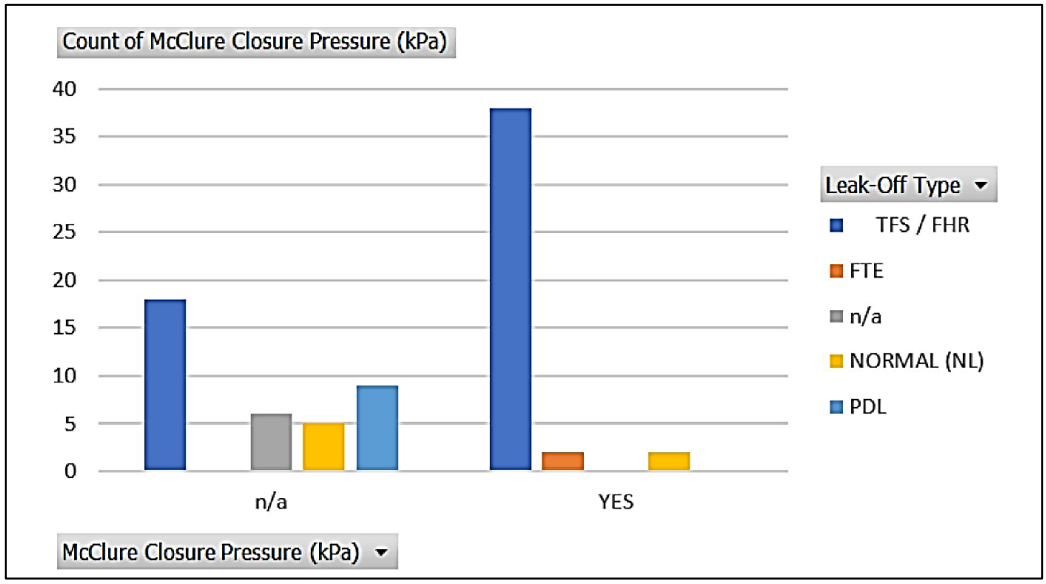

Figure 16. Pivot chart for leak-off types for Canadian Montney Shale Play (Virues et al. (2023)[65]).

Similar results for Canadian Duvernay Shale Play published by Virues et al. (2022) [66]. Figure 17 presents the distribution of tests categorized by the strength of the "compliance" method indication of closure on the dP/dG plot, encompassing all 83 tests conducted in the Duvernay formation. The results indicate that 22% of the tests showed a strong indication of closure (green), 23% demonstrated adequate indication (yellow), 14% revealed weak indication (orange), and 41% exhibited no indication of closure (red). This distribution highlights that more than half of the tests (55%) either showed weak or no indication of closure, while less than half (45%) displayed strong or adequate indications of closure.

All those observations are confirmed with the decrease in accuracy of fracture closure detected using the compliance method against the measured rock deformation closure pressure using strain gauges with an increase of natural fractures as seen in Table 2.

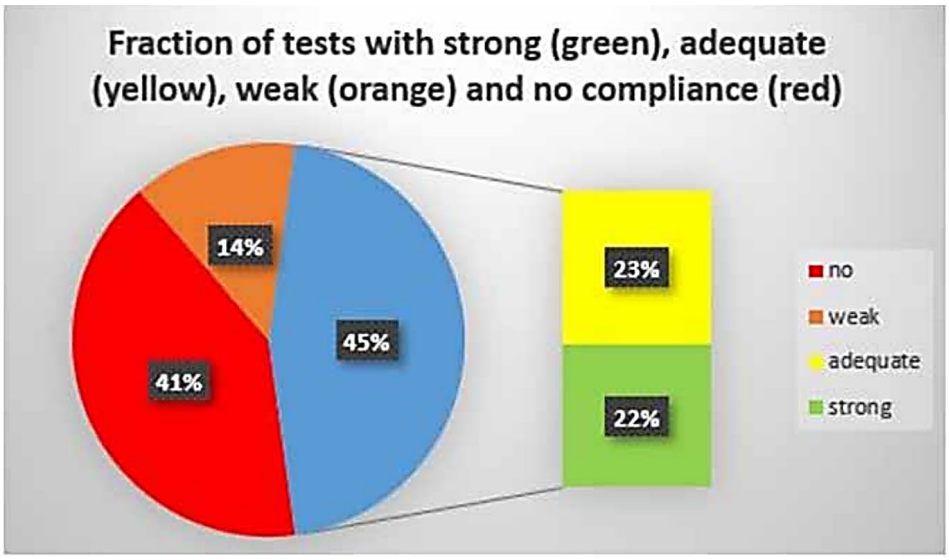

Figure 17. Fraction of tests with strong (green), adequate (yellow), weak (orange), and no (red) compliance indication of closure for Canadian Duvernay Shale Play (Virues et al. (2022)[66]).

Kamali et al. (2019)[67] revealed that the pressure profiles and semi-log G derivatives in their study diverge from those observed in conventional hydraulic fractures, primarily due to stiffness changes within the system. These alterations manifest as distinct patterns on the G-function plot, necessitating caution during closure pressure interpretation to avoid erroneous conclusions. Their

 doi:10.20944/preprints202408.0725.v1

simulations highlight the potential for misidentifying natural fracture closure signatures as closure pressure. Distinguishing between genuine stiffness indicators and data noise proves challenging in field applications. The field example demonstrated that the GdP/dG typically exhibits ideal leak-off behavior, maintaining a linear trajectory until a notable deviation. The discrepancy observed between simulation outcomes and actual field data—namely, the lack of stiffness signatures in the latter—suggests two possible explanations: either the closure mechanism presumed by the stiffness/compliance method deviates from the actual fracture closure mechanism or the hydraulic fracture's stiffness is insufficient to significantly alter system stiffness post-closure. Consequently, the diagnostic plots' stiffness signatures may stem from the closure of intersecting natural fractures.

Employing conventional tangent methods or log-log diagnostic plots in conjunction with the stiffness/compliance method may offer a more reliable means of identifying closure pressure within naturally fractured reservoirs. From previous reviews and mathematical models, we can conclude that no one methodology may be used always successfully to detect fracture closure. However, integration between methodologies should be followed. It is essential to identify the source of permeability and the degree of natural fracture intensity to select the most appropriate model for detecting fracture closure. Generic methodologies, such as the continuous wavelet transform (CWT) fracture closure detection technique, should be employed to determine the most reliable methodology.

If natural fracture or transverse storage leak-off behavior are the primary types of leak-off permeability and are likely to affect system stiffness restoration during the closure process, tangent method models (either transverse storage or pressure-dependent leak-off behavior) are the most suitable. These models can be extensively analyzed to estimate the volume of natural fractures or transverse storage laminas.

Gabry et al. (2023b) [48] demonstrated that fracture closure measured using rock deformation strain gauges was sometimes consistent with the compliance method and other times with tangent methods, depending on the similarity between the technique model assumptions and the actual rock status. Each methodology has its own set of assumptions, while the continuous wavelet transform (CWT) technique serves as a generic method based on a mathematical microscope. However, the CWT fracture closure detection technique provides a generic analysis to detect the fracture closure without any pre-assumptions or simplification.

7. Conclusions

From the previous review and discussions, we can conclude the following: -

- Disturbances in flow periods, particularly during post-closure pseudo-linear and pseudo-radial periods, significantly affect the interpretation of fracture closure pressure using the tangent method.
- In naturally fractured reservoirs, there is no significant increase in system stiffness post-closure due to residual apertures remaining after disturbance. Higher fracture permeability results in lower system stiffness, and as a result, DFITs in these reservoirs, initially in equilibrium with natural fractures, do not exhibit an observable increase in system stiffness, rendering the compliance method ineffective for detecting fracture closure in this scenario.
- The tangent method is crucial for identifying different leak-off regimes, which are essential for fracture closure detection. Recognizing the source of leak-off permeability, understanding rock properties, and assessing natural fracture intensity is vital for selecting the most appropriate model for detecting fracture closure. Tangent method models may be used to analyze naturally fractured reservoirs and estimate the volume of natural fractures or transverse storage laminas. The tangent method is influenced by disturbances in the flow regime after fracture closure, which may cause a monotonic increase in the GdP/dG vs. G time plot during field application.
- The compliance method can enhance reservoir evaluation by assessing system stiffness. Combining both the tangent and compliance methods, along with the continuous wavelet transform (CWT) fracture closure detection technique, offers a more reliable approach to identifying fracture closure.

- The CWT fracture closure detection technique provides a powerful analysis technique to detect fracture closure without any pre-assumptions or simplification, as it is based on data analysis. The CWT technique can detect all features embedded in DFIT shut-in pressure.

Author Contributions: Conceptualization, M.A.G.; methodology, M.A.G.; software, A.G.; validation, I.E.; formal analysis, I.E.; writing—review and editing, A.R.; visualization, A.R.; supervision, M.Y.S.; project administration, M.Y.S.; funding acquisition, M.Y.S. All authors have read and agreed to the published version of the manuscript.".

Conflicts of Interest: The authors declare no conflicts of interest.

Informed Consent Statement: Not applicable.

Funding: This research received no external funding.

References

1. Teufel, L. W.; Clark, J. A. Hydraulic fracture propagation in layered rock: experimental studies of fracture containment. *Soc. Pet. Eng. J.* 1984, 24, 19–32.
2. Hubbert, M. K.; Willis, D. G. Mechanics of hydraulic fracturing. *Trans. AIME* 1957, 210, 153–168.
3. Godbey, J. K.; Hodges, H. D. Pressure measurements during formation fracturing operations. *Trans. AIME* 1958.
4. Kehle, R. O. The determination of tectonic stresses through analysis of hydraulic well fracturing. *J. Geophys. Res.* 1964, 69, 259–273.
5. Haimson, B.; Fairhurst, C. Initiation and extension of hydraulic fractures in rocks. *Soc. Pet. Eng. J.* 1967, 7, 310–318.
6. Zoback, M. D.; Hickman, S. In situ study of the physical mechanisms controlling induced seismicity at Monticello Reservoir, South Carolina. *J. Geophys. Res.: Solid Earth* 1982, 87, 6959–6974.
7. McLennan, J. D.; Roegiers, J. C. How instantaneous are instantaneous shut-in pressures? In *Proceedings of the SPE Annual Technical Conference and Exhibition*, New Orleans, LA, USA, 26–29 September 1982; Society of Petroleum Engineers: 1982; pp. SPE-11064.
8. Mayerhofer, M. J.; Economides, M. J. Permeability estimation from fracture calibration treatments. In *Proceedings of the SPE Western Regional Meeting*, Anchorage, AK, USA, 26–28 May 1993; Society of Petroleum Engineers: 1993; pp. SPE-26039.
9. Nolte, K. G. Determination of fracture parameters from fracturing pressure decline. In *Proceedings of the SPE Annual Technical Conference and Exhibition*, Las Vegas, NV, USA, 23–26 September 1979; Society of Petroleum Engineers: 1979; pp. SPE-8341.
10. Mayerhofer, M. J.; Economides, M. J. Permeability Estimation From Fracture Calibration Treatments. Paper presented at the *SPE Western Regional Meeting*, Anchorage, Alaska, May 1993. doi: https://doi.org/10.2118/26039-MS.
11. Mayerhofer, M. J.; Ehlig-Economides, C. A.; Economides, M. J. Pressure transient analysis of fracture calibration tests. *J. Pet. Technol.* 1995, 47, 229–234.
12. Craig, D. P.; Brown, T. D. Estimating pore pressure and permeability in massively stacked lenticular reservoirs using diagnostic fracture-injection tests. In *Proceedings of the SPE Annual Technical Conference and Exhibition*, Houston, TX, USA, 3–6 October 1999; Society of Petroleum Engineers: 1999; pp. SPE-56600.
13. Smith, M. B. *Hydraulic Fracturing*; CRC Press: Boca Raton, FL, USA, 2015.
14. Theis, C. V. The relation between the lowering of the piezometric surface and the rate and duration of discharge of a well using ground-water storage. *Trans. Am. Geophys. Union* 1935, 16, 519–524.
15. Horne, R.; Temeng, K. O. Relative productivities and pressure transient modeling of horizontal wells with multiple fractures. In *Proceedings of the SPE Middle East Oil and Gas Show and Conference*, Manama, Bahrain, 11–14 March 1995; Society of Petroleum Engineers: 1995; pp. SPE-29891.
16. Castillo, J. L. Modified fracture pressure decline analysis including pressure-dependent leakoff. In *Proceedings of the SPE Rocky Mountain Petroleum Technology Conference/Low-Permeability Reservoirs Symposium*, Denver, CO, USA, 27–29 May 1987; Society of Petroleum Engineers: 1987; pp. SPE-16417.
17. Barree, R. D.; Mukherjee, H. Determination of pressure-dependent leakoff and its effect on fracture geometry. In *Proceedings of the SPE Annual Technical Conference and Exhibition*, Denver, CO, USA, 6–9 October 1996; Society of Petroleum Engineers: 1996. https://doi.org/10.2118/36424-MS.
18. Barree, R. D.; Barree, V. L.; Craig, D. P. Holistic fracture diagnostics. In *Proceedings of the Rocky Mountain Oil & Gas Technology Symposium*, Denver, CO, USA, 17–19 April 2007; Society of Petroleum Engineers: 2007. https://doi.org/10.2118/107877-MS.
19. Barree, R. D.; Barree, V. L.; Craig, D. P. Holistic fracture diagnostics: consistent interpretation of prefrac injection tests using multiple analysis methods. *SPE Prod. Oper.* 2009, 24 (3), 396–406.

20. McClure, M. W.; Blyton, C. A.; Jung, H.; Sharma, M. M. The effect of changing fracture compliance on pressure transient behavior during diagnostic fracture injection tests. In *Proceedings of the SPE Annual Technical Conference and Exhibition*, Amsterdam, The Netherlands, 27–29 October 2014; Society of Petroleum Engineers: 2014. https://doi.org/10.2118/170956-MS.
21. McClure, M. W.; Jung, H.; Cramer, D. D.; Sharma, M. M. The fracture-compliance method for picking closure pressure from diagnostic fracture-injection tests. SPE J. 2016, 21, 1321-1339. https://doi.org/10.2118/179725-PA
22. Jung, H.; Sharma, M. M.; Cramer, D. D. Re-examining interpretations of non-ideal behavior during diagnostic fracture injection test. J. Pet. Sci. Eng. 2016, 145, 114-136. https://doi.org/10.1016/j.petrol.2016.03.016
23. Wang, H.; Sharma, M. M. New variable compliance method for estimating in-situ stress and leak-off from DFIT data. In Proceedings of the SPE Annual Technical Conference and Exhibition, San Antonio, TX, USA, 9-11 October 2017; Society of Petroleum Engineers, 2017. https://doi.org/10.2118/187348-MS
24. Gu, H.; Leung, K. H. 3D numerical simulation of hydraulic fracture closure with application to mini-fracture analysis. J. Pet. Technol. 1993, 45, 206-255.
25. Soliman, M. Y.; Craig, D.; Bartko, K.; Rahim, Z.; Adams, D. After-closure analysis to determine formation permeability, reservoir pressure, and residual fracture properties. In Proceedings of the SPE Middle East Oil and Gas Show and Conference, Manama, Bahrain, 12-15 March 2005; Society of Petroleum Engineers, 2005; pp. SPE-93419.
26. Craig, D. P.; Blasingame, T. A. Application of a new fracture-injection/falloff model accounting for propagating, dilated, and closing hydraulic fractures. In Proceedings of the SPE Unconventional Resources Conference/Gas Technology Symposium, Denver, CO, USA, 7-9 February 2006; Society of Petroleum Engineers, 2006; pp. SPE-100578.
27. Nolte, K. G.; Maniere, J. L.; Owens, K. A. After-closure analysis of fracture calibration tests. In Proceedings of the SPE Annual Technical Conference and Exhibition, San Antonio, TX, USA, 5-8 October 1997; Society of Petroleum Engineers, 1997; pp. SPE-38676.
28. Gulrajani, S. N.; Nolte, K. G.; Economides, M. J. Fracture evaluation using pressure diagnostics. Reservoir Stimulation 2000, 9.
29. McClure, M. W.; Jung, H.; Cramer, D. D.; Sharma, M. M. The fracture-compliance method for picking closure pressure from diagnostic fracture-injection tests. SPE J. 2016, 21, 1321-1339.
30. Bruno, J.; Sun, H.; Yu, W.; Sepehrnoori, K. New diagnostic fracture injection test model with complex natural fractures using embedded discrete fracture model. In Proceedings of the ARMA US Rock Mechanics/Geomechanics Symposium, Houston, TX, USA, 20-23 June 2021; American Rock Mechanics Association, 2021; pp. ARMA-2021.
31. Howard, G. C.; Fast, C. R. Optimum fluid characteristics for fracture extension. Drilling and Production Practice 1957.
32. Barree, R. D.; Miskimins, J. L. Physical explanation of non-linear derivatives in diagnostic fracture injection test analysis. In Proceedings of the SPE Hydraulic Fracturing Technology Conference, The Woodlands, TX, USA, 9-11 February 2016; Society of Petroleum Engineers, 2016. https://doi.org/10.2118/179134-MS
33. Liao, C.; Wang, R.; Zhang, J.; Huang, Q.; Li, X.; Zheng, X.; Lin, Z. Well testing analysis methodology and application for complex fault-block reservoirs in the exploration stage. In Proceedings of the SPE Gas & Oil Technology Showcase and Conference, Dubai, UAE, 13-15 March 2023; Society of Petroleum Engineers, 2023; pp. D021S028R006.
34. Han, G.; Bartko, K.; Mutlu, U. Geomechanical, geological, and engineering controls of hydraulic fracturing. In Proceedings of the Unconventional Resources Technology Conference (URTeC), Denver, CO, USA, 22-24 July 2019; Aramco Services Company, Saudi Aramco, Rockfield Global Technologies. https://doi.org/10.15530/urtec-2019-34
35. McClure, M. The spurious deflection on log-log superposition-time derivative plots of diagnostic fracture-injection tests. SPE Reserv. Eval. Eng. 2017, 20, 1045-1055. https://doi.org/10.2118/186098-PA
36. Sneddon, I. N. The distribution of stress in the neighborhood of a crack in an elastic solid. Proc. R. Soc. Lond. A Math. Phys. Sci. 1946, 187, 229-260.
37. Barton, N.; Bandis, S. C.; Bakhtar, K. Strength, deformation and conductivity coupling of rock joints. Int. J. Rock Mech. Min. Sci. Geomech. Abstr. 1985, 22, 121-140.
38. Willis-Richards, J.; Watanabe, K.; Takahashi, H. Progress toward a stochastic rock mechanics model of engineered geothermal systems. J. Geophys. Res.: Solid Earth 1996, 101, 17481-17496.
39. McClure, M. Discussion of the paper SPE-187038-MS: Fracture closure stress: Reexamining field and laboratory experiments of fracture closure using modern interpretation methodologies. arXiv preprint arXiv:1904.07126, 2019.
40. McClure, M.; Albrecht, M.; Cipolla, C.; Molina, C. Design and implementation of field tests in unconventional reservoirs: Practical perspectives. In Proceedings of the SPE Annual Technical Conference

and Exhibition, Houston, TX, USA, 3-5 October 2022; Society of Petroleum Engineers, 2022; pp. D011S016R005.
41. Soliman, M. Y.; Ansah, J.; Stephenson, S.; Mandal, B. Application of wavelet transform to analysis of pressure transient data. In Proceedings of the SPE Annual Technical Conference and Exhibition, New Orleans, LA, USA, 30 September-3 October 2001; Society of Petroleum Engineers, 2003.
42. Soliman, M. Y.; Stephenson, S. Methods for combining well test analysis with wavelet analysis. U.S. Patent 6,347,283.
43. Soliman, M. Y.; Ansah, J. Methods and systems for using wavelet analysis in subterranean applications. U.S. Patent 6,978,211.
44. Unal, E.; Siddiqui, F.; Soliman, M. Y.; Dindoruk, B. Wavelet analysis of DFIT data to identify fracture closure parameters. In Proceedings of the SPE Hydraulic Fracturing Technology Conference and Exhibition, The Woodlands, TX, USA, 5-7 February 2019; Society of Petroleum Engineers, 2019. https://doi.org/10.2118/194326-MS
45. Eltaleb, I.; Rezaei, A.; Siddiqui, F.; Awad, M. M.; Mansi, M.; Dindoruk, B.; Soliman, M. Y. Analysis of fracture injection tests using signal processing approach. In Proceedings of the SPE/AAPG/SEG Unconventional Resources Technology Conference, Virtual, 20-22 July 2020; Society of Petroleum Engineers, 2020. https://doi.org/10.15530/urtec-2020-3183
46. Eltaleb, I.; Rezaei, A.; Soliman, M. Y.; Dindoruk, B. A signal processing approach for analysis of fracture injection test in geothermal reservoirs: A case study on the Utah FORGE formation. In Proceedings of the SPE Hydraulic Fracturing Technology Conference and Exhibition, Virtual, 18-19 May 2021; Society of Petroleum Engineers, 2021. https://doi.org/10.2118/204164-MS
47. Gabry, M. A.; Eltaleb, I.; Soliman, M. Y.; Farouq-Ali, S. M. A new technique for estimating stress from fracture injection tests using continuous wavelet transform. Energies 2023, 16, 764.
48. Gabry, M. A.; Eltaleb, I.; Soliman, M. Y.; Farouq-Ali, S. M. Validation of estimating stress from fracture injection tests using continuous wavelet transform with experimental data. Energies 2023, 16, 2807.
49. Craig, D. P. New type curve analysis removes limitations of conventional after-closure analysis of DFIT data. In Proceedings of the SPE Unconventional Resources Conference/Gas Technology Symposium, The Woodlands, TX, USA, 1-3 April 2014; Society of Petroleum Engineers, 2014; pp. D031S007R006.
50. Jung, H.; Sharma, M. M.; Cramer, D. D. Enhanced diagnostic fracture injection test analysis using advanced wavelet transform techniques. In Proceedings of the SPE Annual Technical Conference and Exhibition, San Antonio, TX, USA, 9-11 October 2017; Society of Petroleum Engineers, 2017; pp. SPE-187746-MS.
51. van den Hoek, P. A simple unified pressure-transient-analysis method for fractured waterflood injectors and mini fractures in hydraulic-fracture stimulation. SPE Prod. Oper. 2018, 33, 32-48.
52. Siddiqui, F.; Soliman, M. Y.; House, W.; Ibragimov, A. A new analysis technique for interpreting injection/shut-in tests. Hydraul. Fract. Q. 2016.
53. Zanganeh, B.; Clarkson, C. R.; Jones, J. R. Reinterpretation of flow patterns during DFITs based on dynamic fracture geometry, leakoff and afterflow. In Proceedings of the SPE Hydraulic Fracturing Technology Conference and Exhibition, The Woodlands, TX, USA, 23-25 January 2018; Society of Petroleum Engineers, 2018; pp. D031S007R003.
54. Dutler, N.; Valley, B.; Gischig, V.; Jalali, M.; Brixel, B.; Krietsch, H.; Roques, C.; Amann, F. Hydromechanical insight of fracture opening and closure during in-situ hydraulic fracturing in crystalline rock. Int. J. Rock Mech. Min. Sci. 2020, 135, 104450.
55. Gulrajani, S. N.; Nolte, K. G.; Romero, J. Evaluation of the M-Site B-sand fracture experiments: Evolution of a pressure analysis methodology. SPE Prod. Facil. 2001, 16, 30-41.
56. Guglielmi, Y.; McClure, M.; ... & the EGS Collab Team. Estimating stress from fracture injection tests: Comparing pressure transient interpretations with in-situ strain measurements. In Proceedings of the 47th Workshop on Geothermal Reservoir Engineering, Stanford University, Stanford, CA, USA, 7-9 February 2022; pp. SGP-TR 223.
57. Kneafsey, T. J.; Blankenship, D.; Knox, H. A.; Johnson, T. C.; Ajo-Franklin, J. B.; Schwering, P. C.; ... & Doe, T. EGS Collab project: Status and progress. In Proceedings of the 44th Workshop on Geothermal Reservoir Engineering, Stanford University, Stanford, CA, USA, 11-13 February 2019.
58. Kneafsey, T. J.; Blankenship, D.; Dobson, P. F.; Morris, J. P.; White, M. D.; Fu, P.; ... & Valladao, C. The EGS Collab project: Learnings from Experiment 1. In Proceedings of the 45th Workshop on Geothermal Reservoir Engineering, Stanford University, Stanford, CA, USA, 10-12 February 2020.
59. Guglielmi, Y.; Cook, P.; Soom, F.; Schoenball, M.; Dobson, P.; Kneafsey, T. In situ continuous monitoring of borehole displacements induced by stimulated hydrofracture growth. Geophys. Res. Lett. 2021, 48, e2020GL090782.
60. Guglielmi, Y.; Nussbaum, C.; Jeanne, P.; Rutqvist, J.; Cappa, F.; Birkholzer, J. Complexity of fault rupture and fluid leakage in shale: insights from a controlled fault activation experiment. J. Geophys. Res.: Solid Earth 2020, 125, e2019JB017781.

 doi:10.20944/preprints202408.0725.v1

61. Kakurina, M.; Guglielmi, Y.; Nussbaum, C.; Valley, B. In situ direct displacement information on fault reactivation during fluid injection. Rock Mech. Rock Eng. 2020, 53, 4313-4328.
62. Kerr, E.; Barree, R.; Estrada, E. What can you learn from a DFIT on fiber optics? In Proceedings of the SPE Fracturing Technology Conference and Exhibition, The Woodlands, TX, USA, 6-8 February 2024; Society of Petroleum Engineers, 2024; pp. D011S001R003.
63. Zanganeh, B.; Clarkson, C. R.; Jones, J. R. Reinterpretation of fracture closure dynamics during diagnostic fracture injection tests. In Proceedings of the SPE Western Regional Meeting, Garden Grove, CA, USA, 22-26 April 2018; Society of Petroleum Engineers, 2018; pp. D031S007R009.
64. Buijs, H. DFIT: An interdisciplinary validation of fracture closure pressure interpretation across multiple basins. In Proceedings of the SPE Annual Technical Conference and Exhibition, Dubai, UAE, 21-23 September 2021; Society of Petroleum Engineers, 2021; pp. D021S036R006.
65. Virues, C.; Robertson, A.; Sendecki, B. Best practices in DFIT interpretation-comparative analysis of 80 DFITs in the Canadian Montney Shale Play. In Proceedings of the SPE Annual Technical Conference and Exhibition, Calgary, AB, Canada, 25-27 September 2023; Society of Petroleum Engineers, 2023; pp. D031S036R004.
66. Virues, C.; Robertson, A.; AbouKhalil, E. Best practices in DFIT interpretation-comparative analysis of 83 DFITs in the Canadian Duvernay Shale Play. In Proceedings of the SPE Annual Technical Conference and Exhibition, Houston, TX, USA, 3-5 October 2022; Society of Petroleum Engineers, 2022; pp. D021S026R004.
67. Kamali, A.; Ghassemi, A. On the role of poroelasticity in the propagation mode of natural fractures in reservoir rocks. Rock Mech. Rock Eng. 2020, 53, 2419-2438.